The Atacama Cosmology Telescope Sunyaev-Zel'dovich Galaxy Cluster Survey

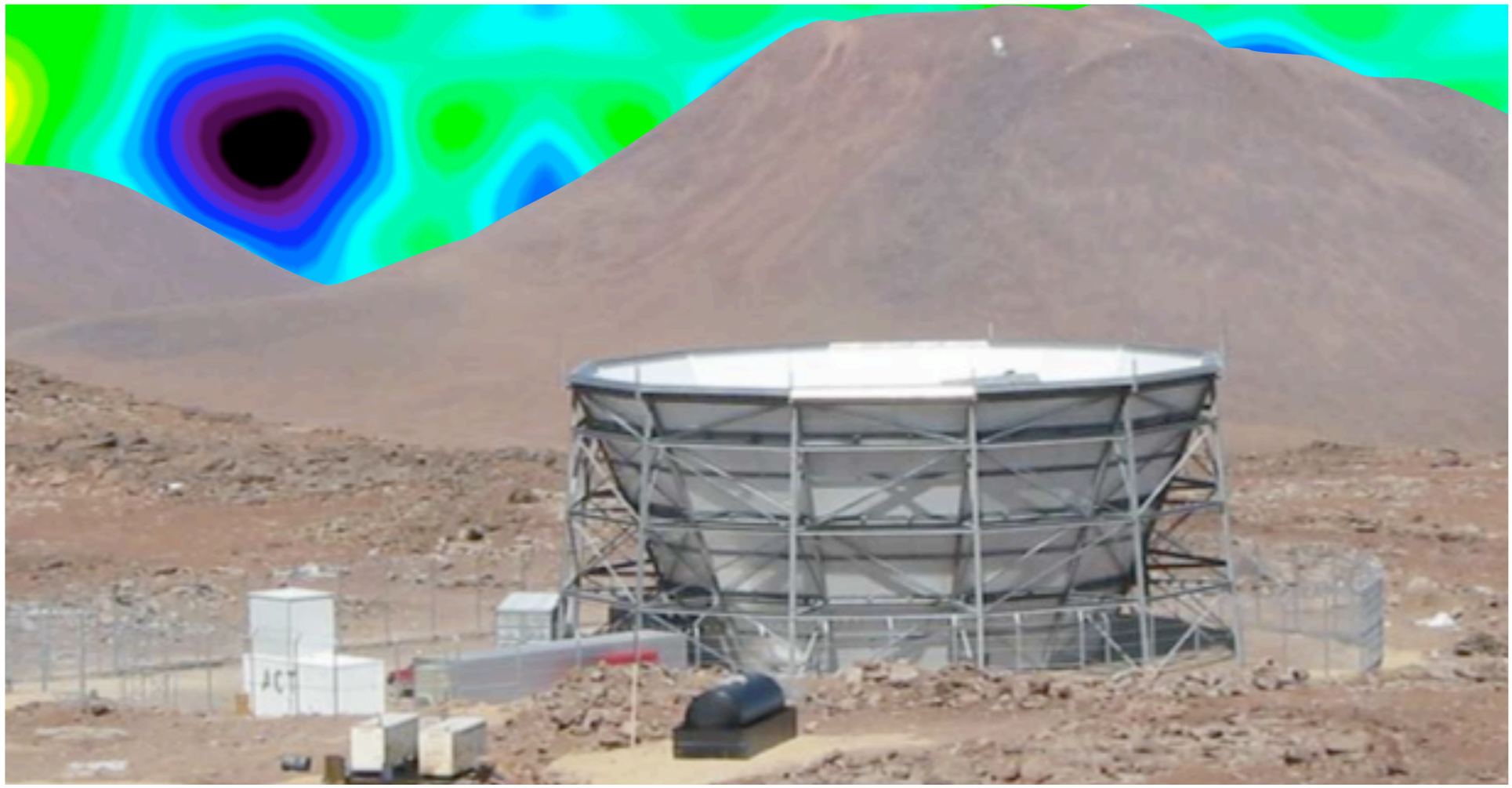

Tobias Marriage (JHU) for the ACT Collaboration

THE UNIVERSE AS SEEN BY PLANCK

ESA/ESTEC, Noodwijk, The Netherlands

April 2-5, 2013

The Site and Telescope

Fowler et al. 2007

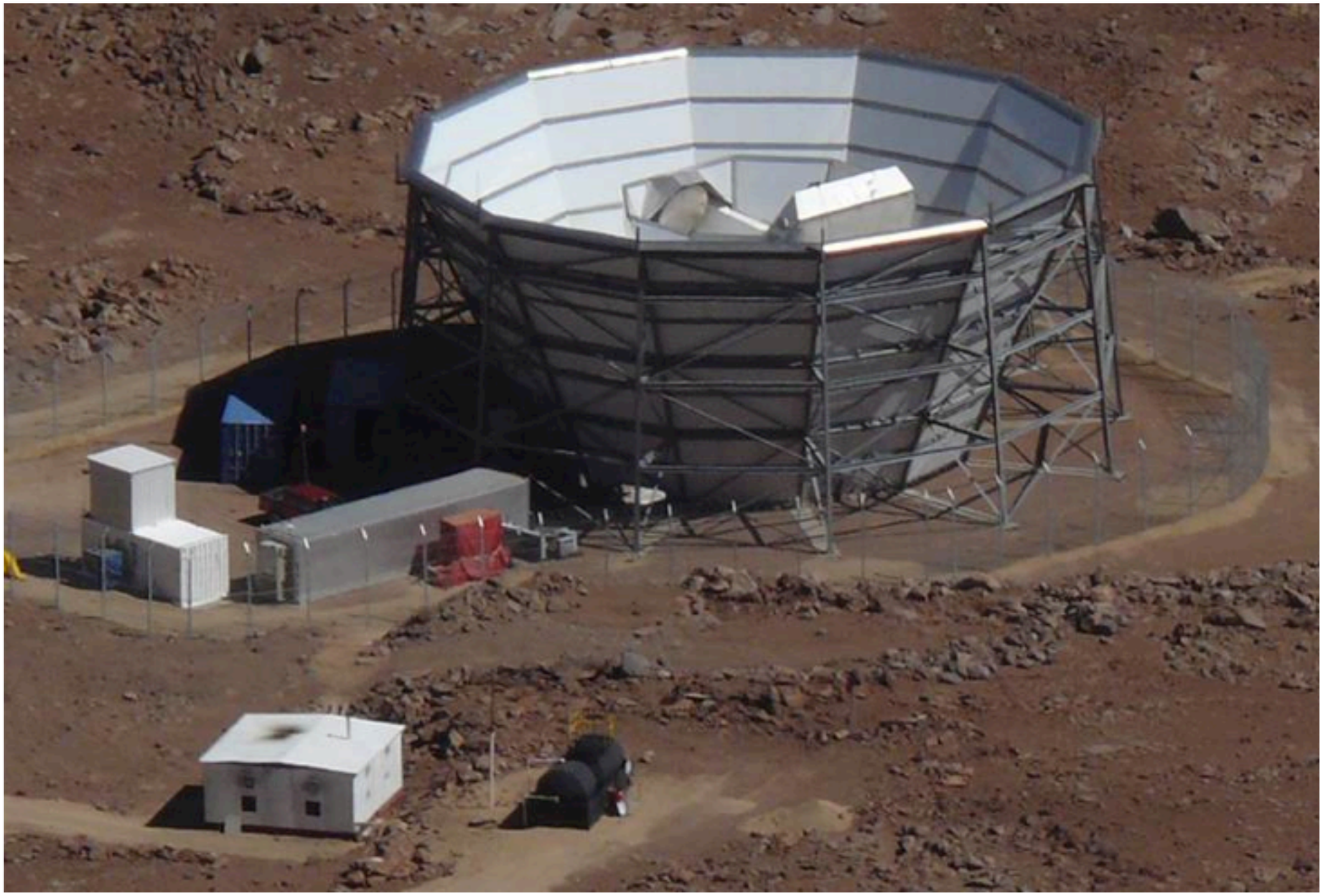

6 meter Survey Telescope at 5200 m Atacama Site (near ALMA)

Not far from the equator: 65% of sky survey-able above 45º elevation.

The Receiver

Swetz et al. 2011 (1007.0290)

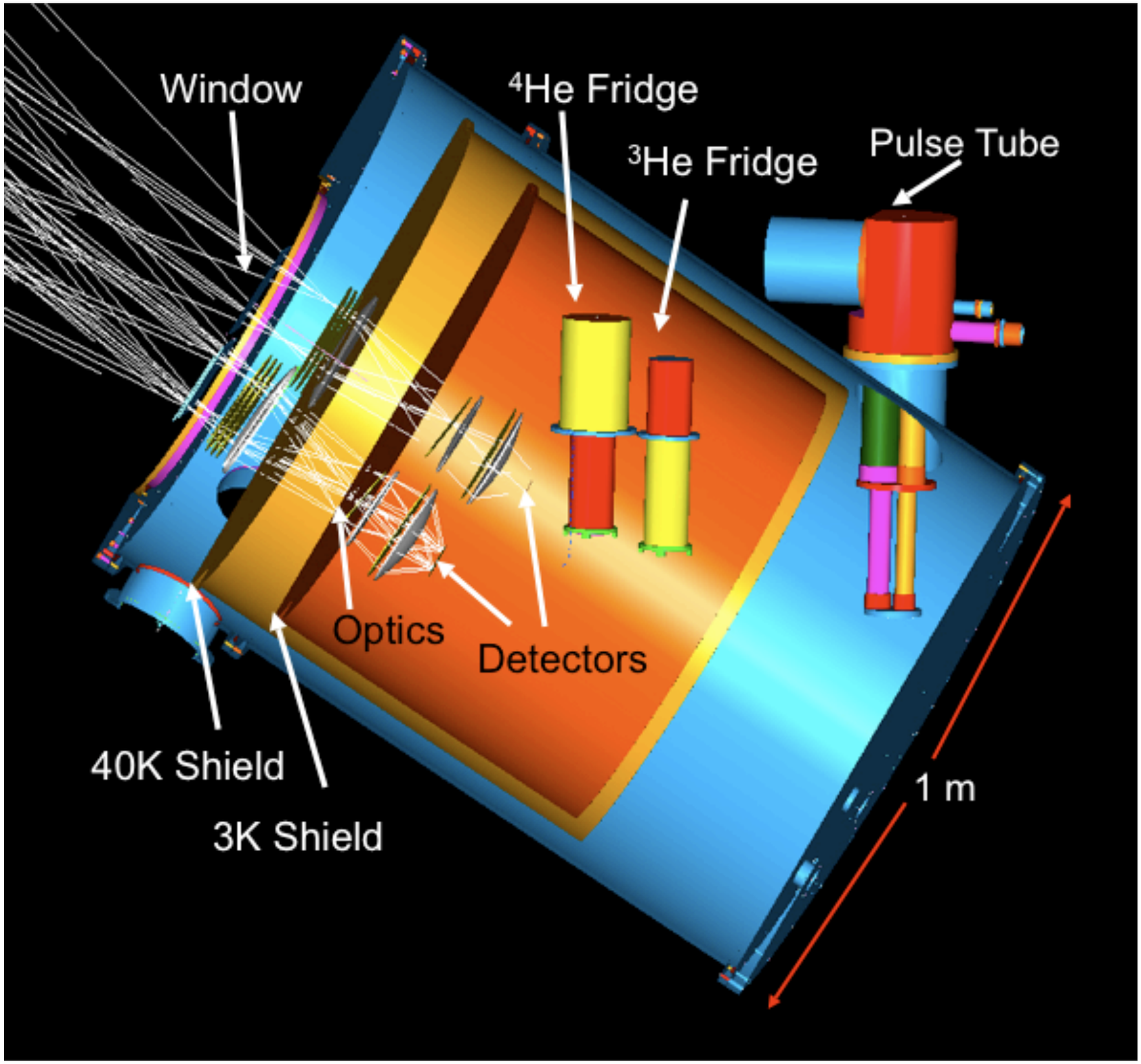

148 GHz

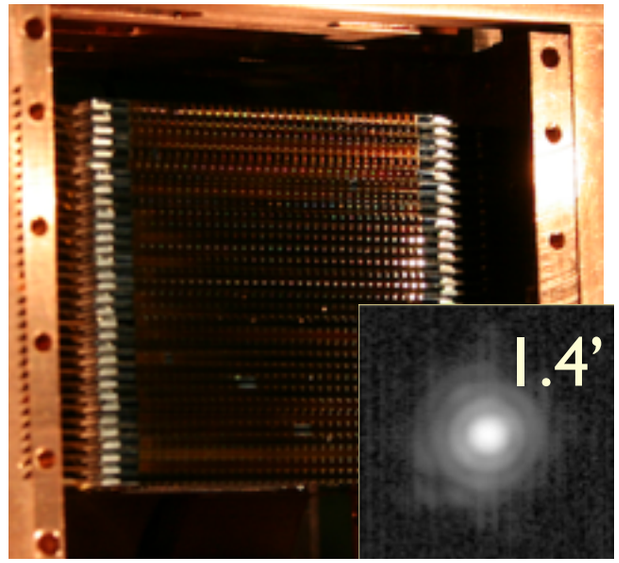

218 GHz

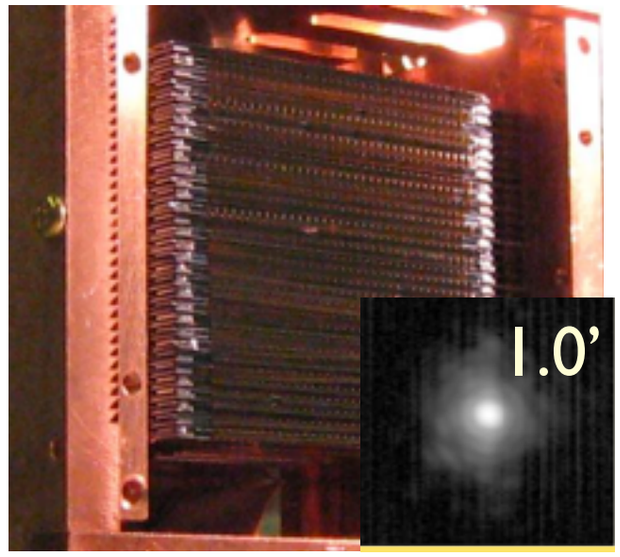

277 GHz

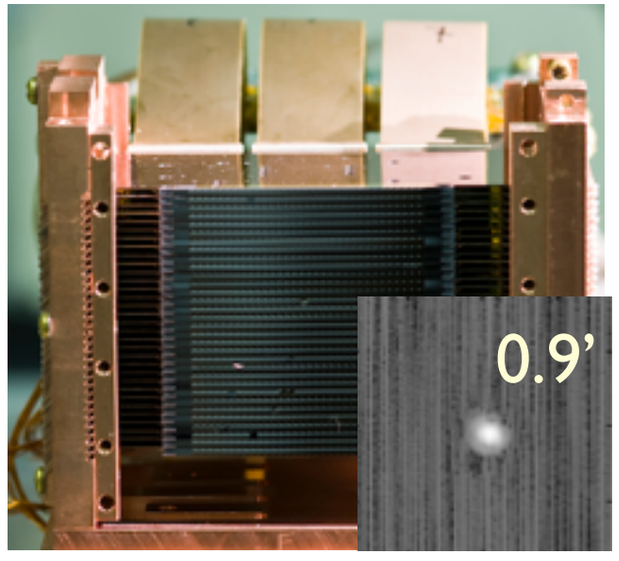

ACT Survey

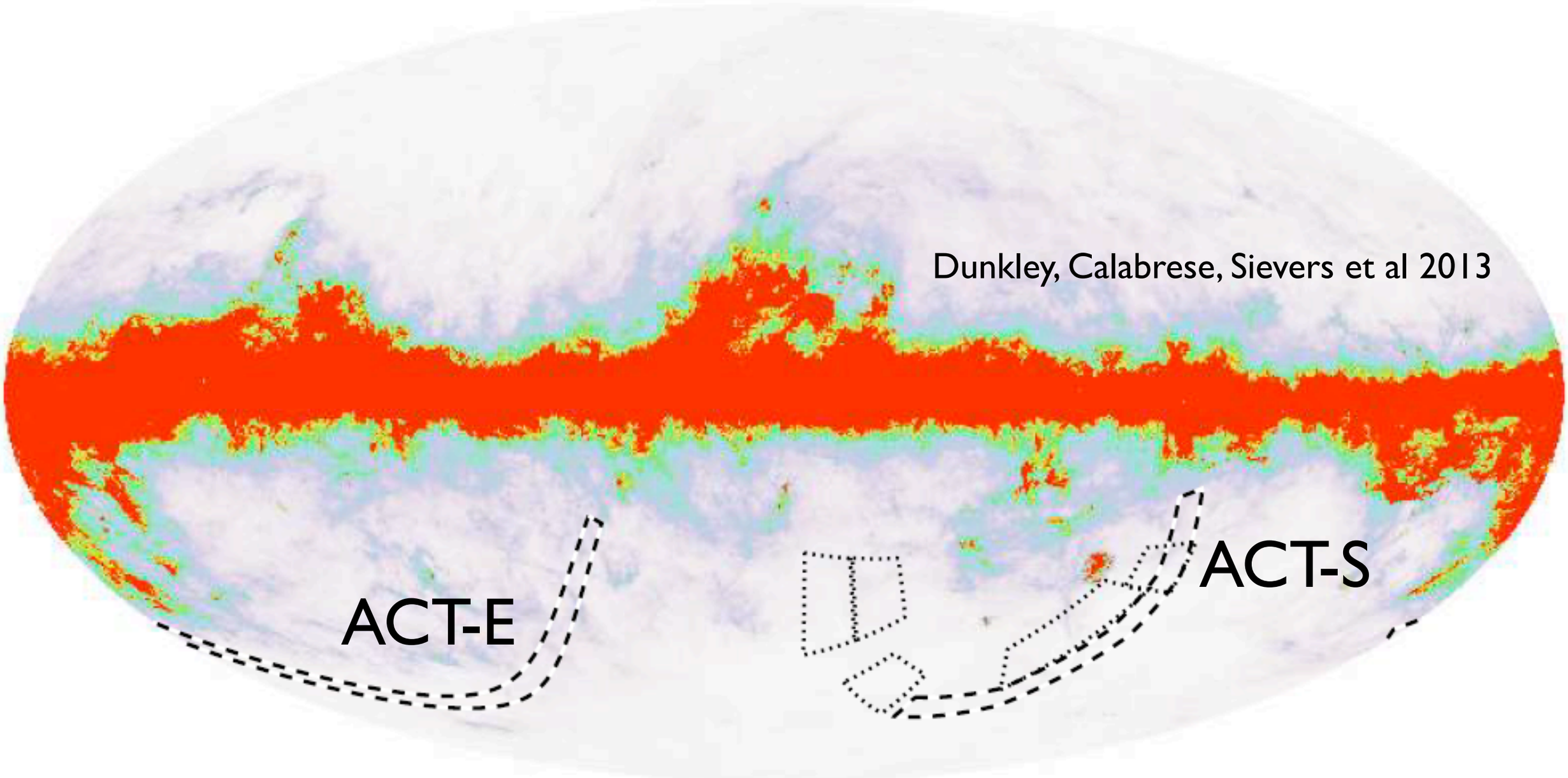

Dashed Regions

ACT-E : 2009-2010; ACT-S 2007-2010

Essentially 1000 sq-deg (950 sq-deg SZ studies)

Dotted Regions are first 800 sq-deg of SPT (out of 2500 sq-deg)

ACT Maps

Signal Recovery from Acoustic Oscillation to Cluster Scales

Dünner, Hasselfield, TM,
Sievers et al 2013

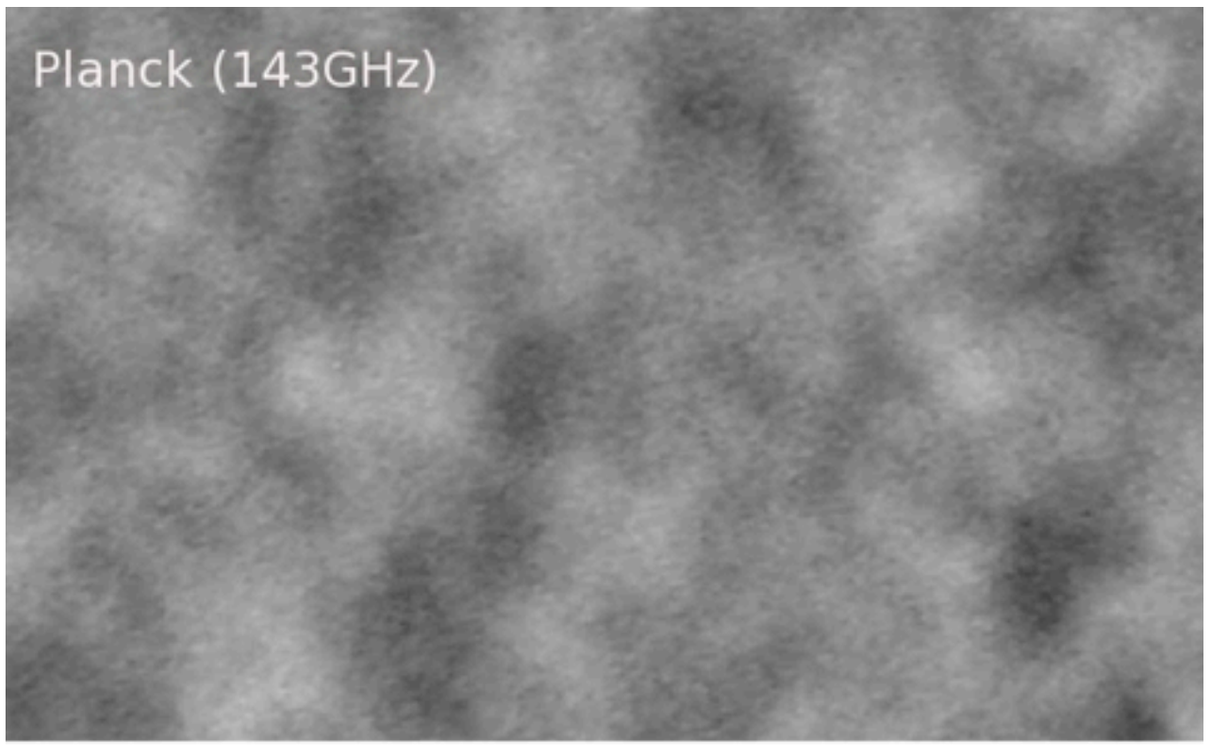

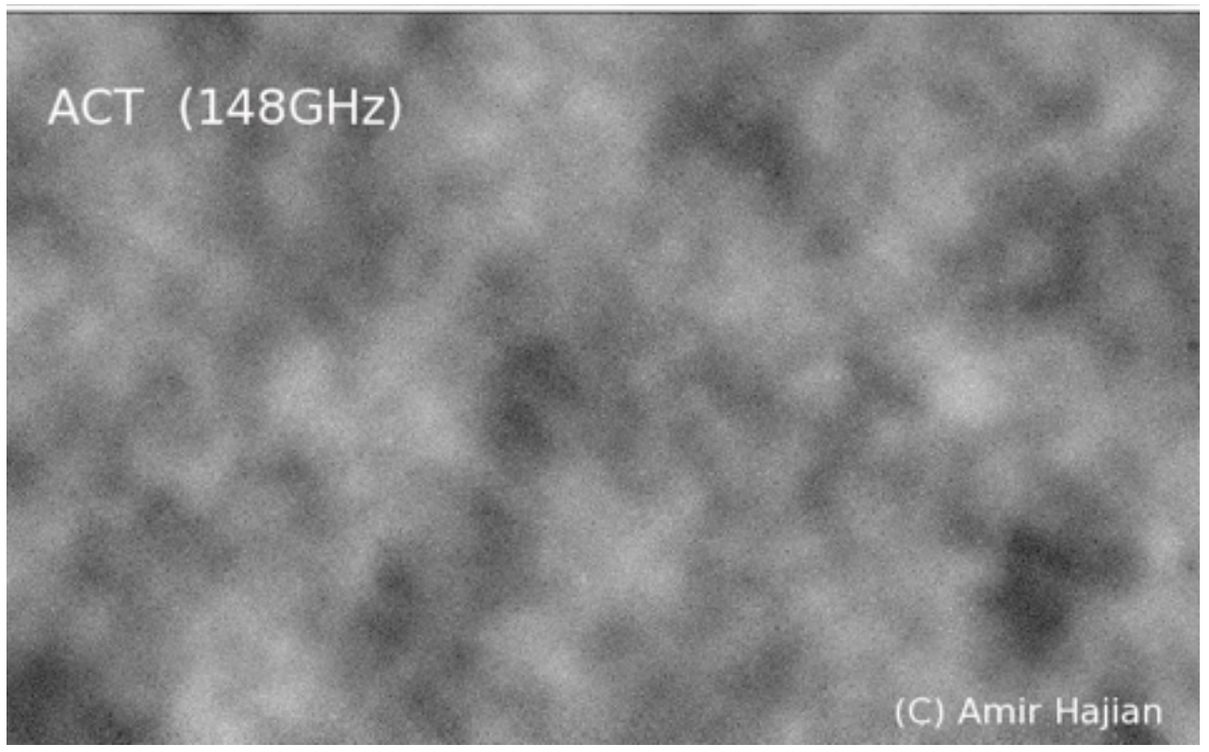

148 GHz, 218 GHz reduced so far;
277 GHz is almost there

Angular Power Spectrum

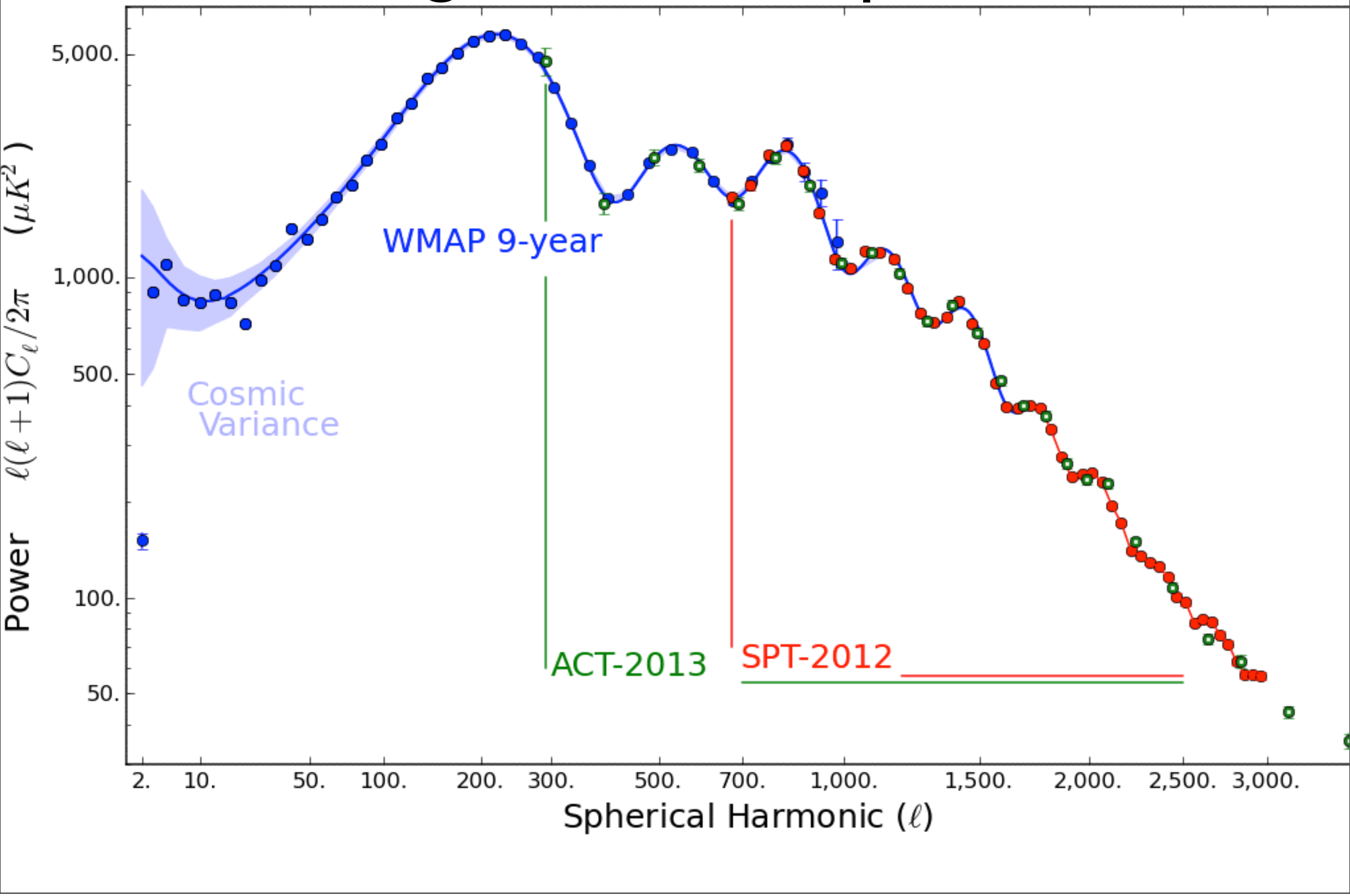

Angular Power Spectrum

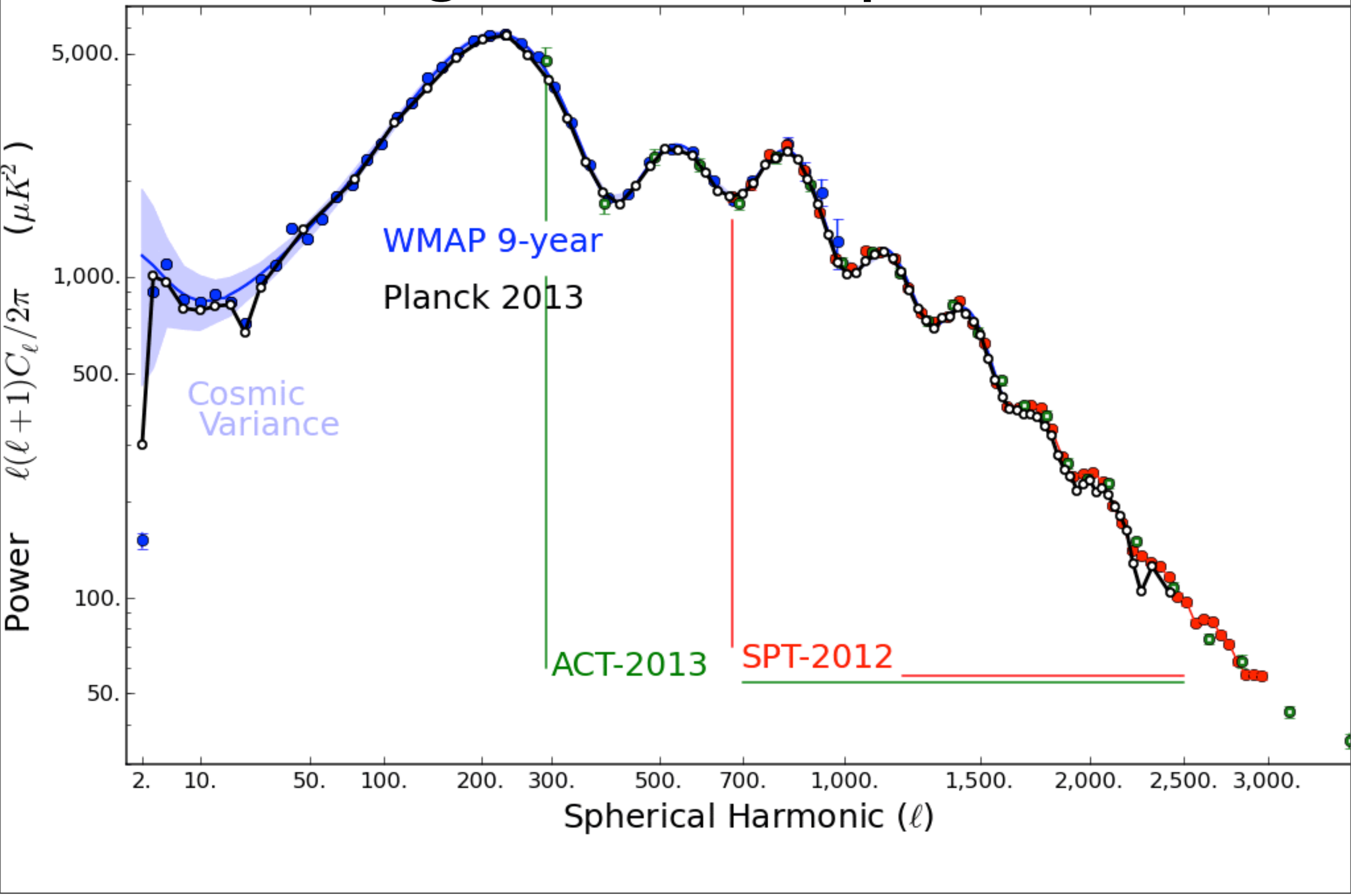

ACT ❤ Planck

CMB Power Spectrum

(Sievers+2013, Calabrese+2013, PXVI 2013)

	WMAP9+ACT	Planck	Planck+WMAP
$100\ \Omega_b h^2$	2.260± 0.041	2.217± 0.033	2.205± 0.028
$100\ \Omega_m h^2$	11.46± 0.43	11.86± 0.31	11.99± 0.27
n_s	0.973± 0.011	0.9635± 0.0094	0.9603± 0.0073
σ_8	0.83± 0.021	0.823± 0.018	0.829± 0.012
H_0	69.7± 2.0	67.9± 1.5	67.3± 1.2

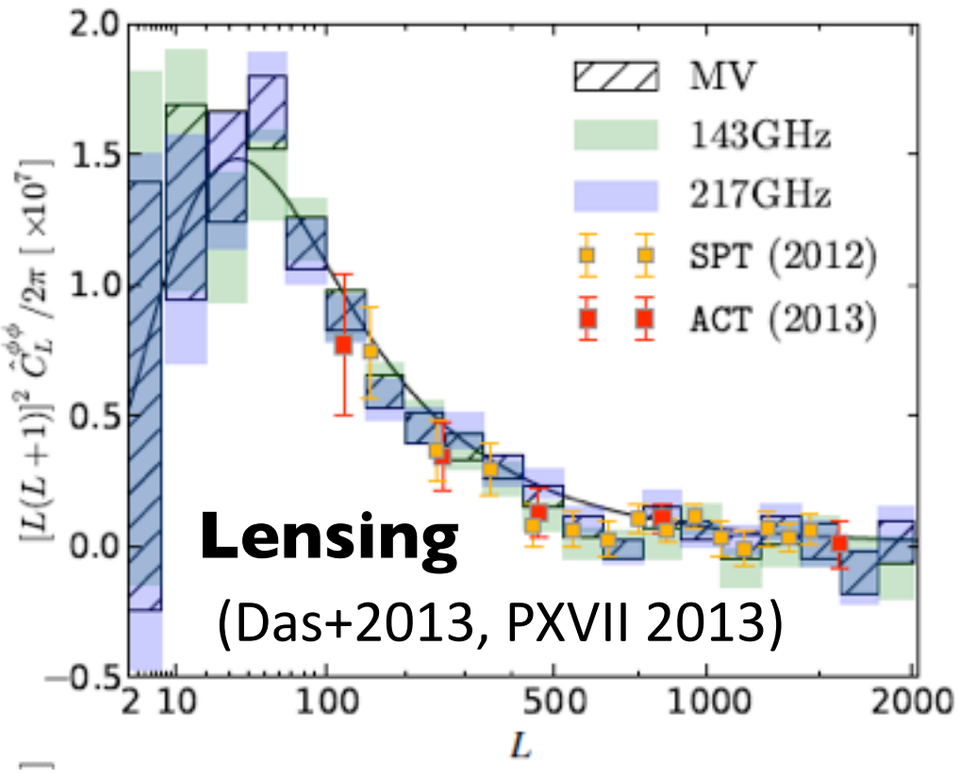

Lensing

(Das+2013, PXVII 2013)

And much more …

tSZ Power Spectrum

ACT: $\sigma_8\ (\Omega_m/.27)^{.3} = 0.77 \pm .06$ (Sievers+2013)

Planck: $\sigma_8\ (\Omega_m/.27)^{3.2/8.1} = 0.78 \pm .016$ (PXXI 2013)

Skewness

ACT: $\sigma_8 = 0.78 \pm 3\%$ stat $\pm 3\%$ sys (Wilson+2012)

Planck: $\sigma_8 = 0.789 \pm .015$ (PXXI 2013)

Source Fluxes

(Gralla+prep, PXXIII 2013)

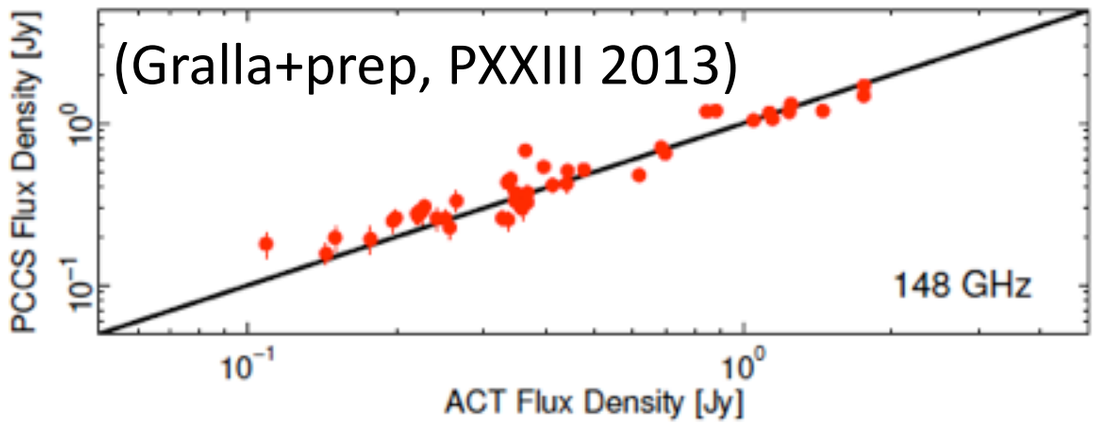

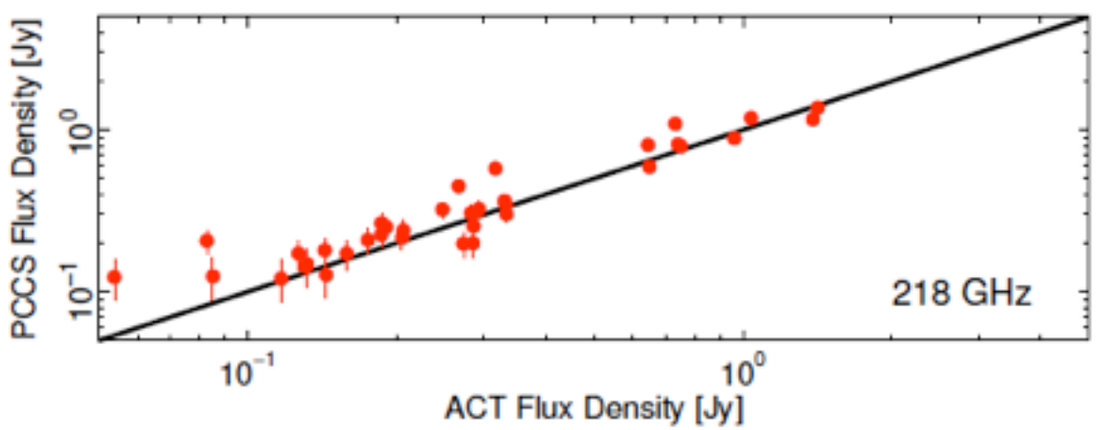

Published ACT Cluster Studies

Southern Survey Clusters

First Look: Hincks et al 2011; SZ Catalog: Marriage et al 2011;
Confirmation+: Menanteau et al 2010; Cosmology: Sehgal et al 2011.

Equatorial Survey Clusters

SZ Catalog & Cosmology: Hasselfield, Hilton, TM et al 2013;
Confirmation+Physical Properties: Menanteau et al 2013.

Multifrequency Studies

Dynamical Masses: Sifon et al 2012; El Gordo: Menanteau et al 2012;
SZA: Reese et al 2011; Subaru: Miyatake et al 2012;
Spitzer: Hilton et al 2013

Stacking Studies with SDSS Stripe 82

LRG tSZ: Hand et al 2011; LRG kSZ: Hand et al 2012;
MaxBCG SZ with mis-centering: Sehgal et al 2012

Related (Beyond Counts)

SZ in PS I: Dunkley et al 2012; SZ in PS II: Sievers et al 2013;
Skewness from SZ: Wilson et al 2012

Cluster Extraction

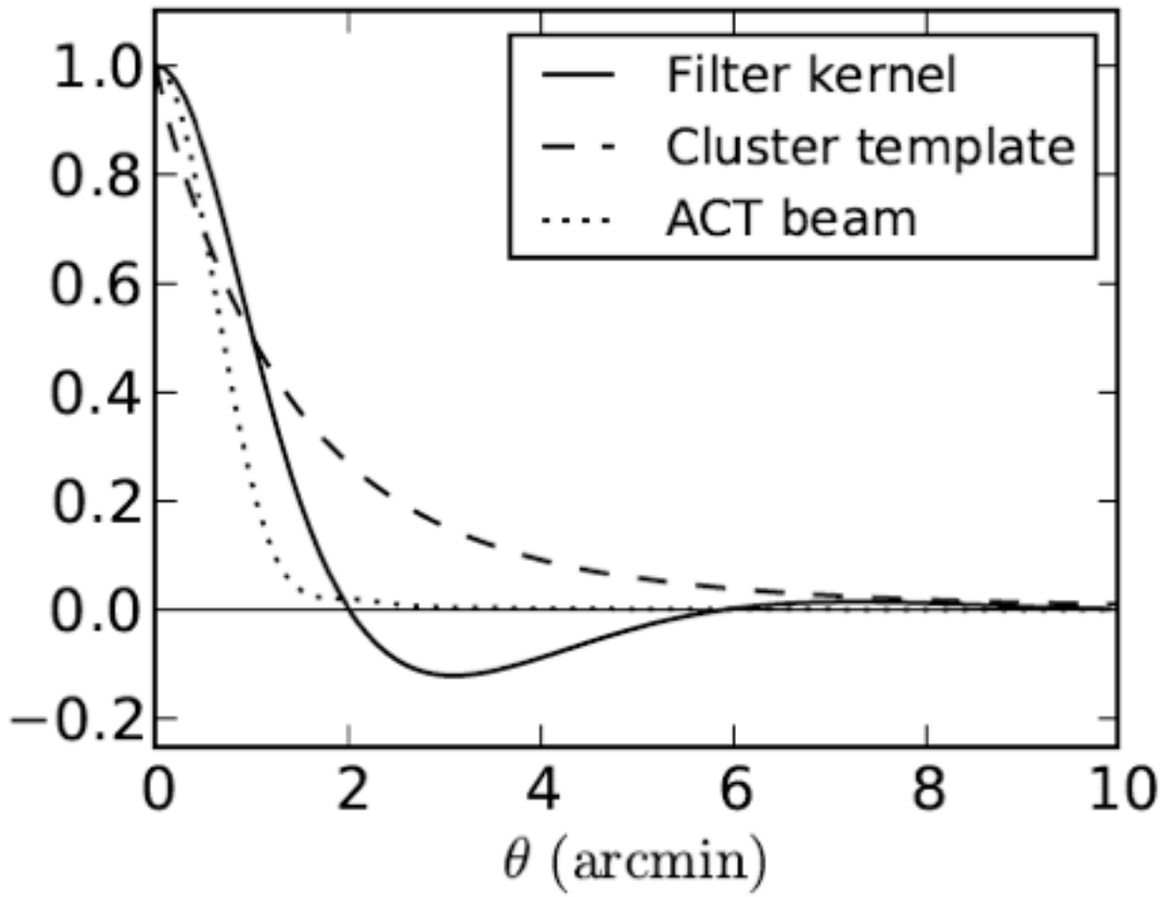

Matched Filter (148 GHz only)

$$\Psi_{\theta_{500}}(\boldsymbol{k}) = \frac{1}{\Sigma_{\theta_{500}}} \frac{B(\boldsymbol{k}) S_{\theta_{500}}(k)}{N(\boldsymbol{k})}$$

Hasselfield, Hilton, Marriage et al 2013

Catalog Results

+68 Blindly Detected Galaxy Clusters; 19 New discoveries

+SZ S/N > 4.0 & Optically Confirmed

+504 sq-deg total (270 sq-deg in SDSS Stripe 82)

With Southern Sample: 91 total published SZ-selected Clusters

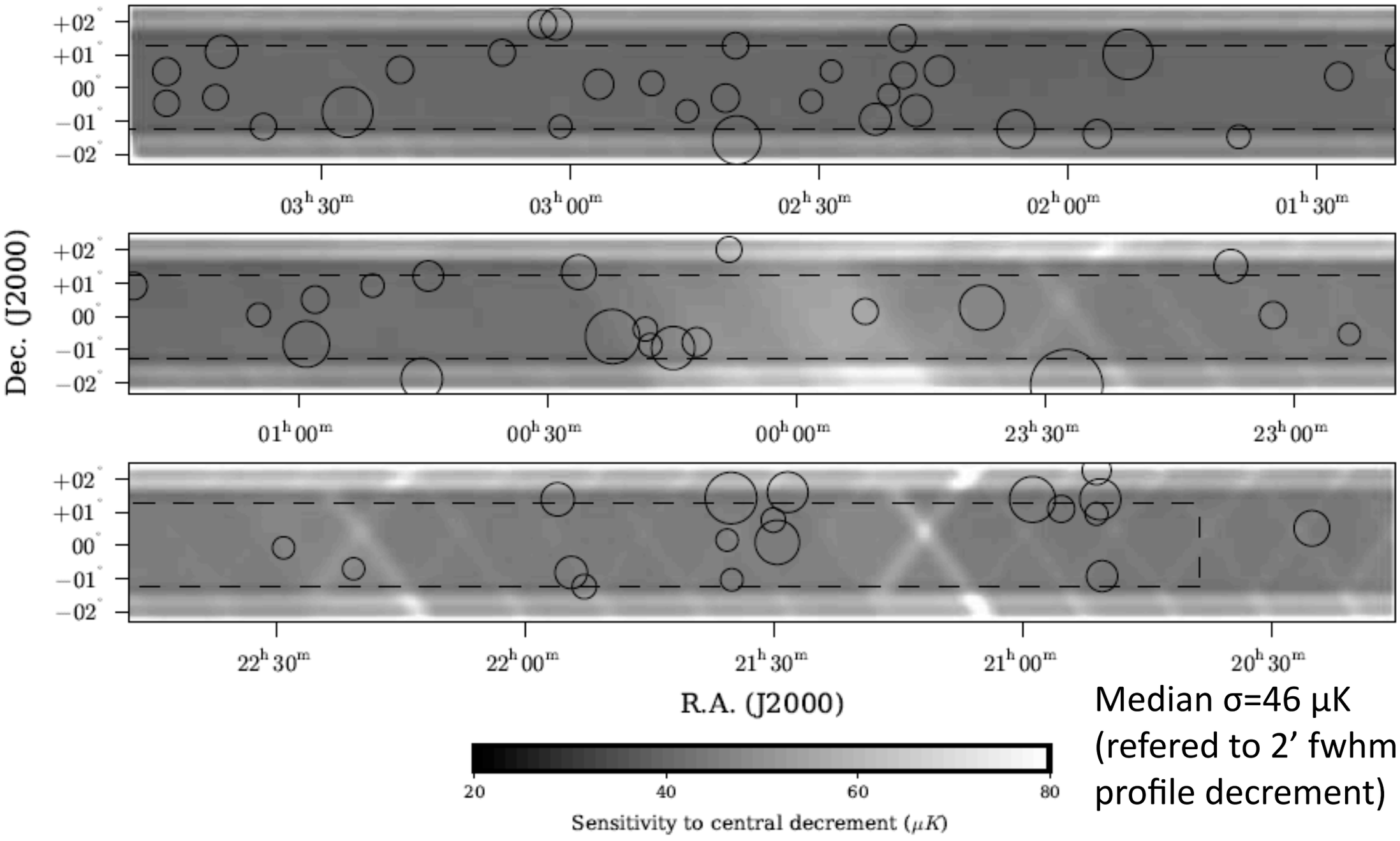

Median σ=46 μK (refered to 2’ fwhm profile decrement)

Optical Confirmation

SDSS and APO 3.5m

Contours are equi-spaced betwee Min/Max SZ decrement

Menanteau et al 2013

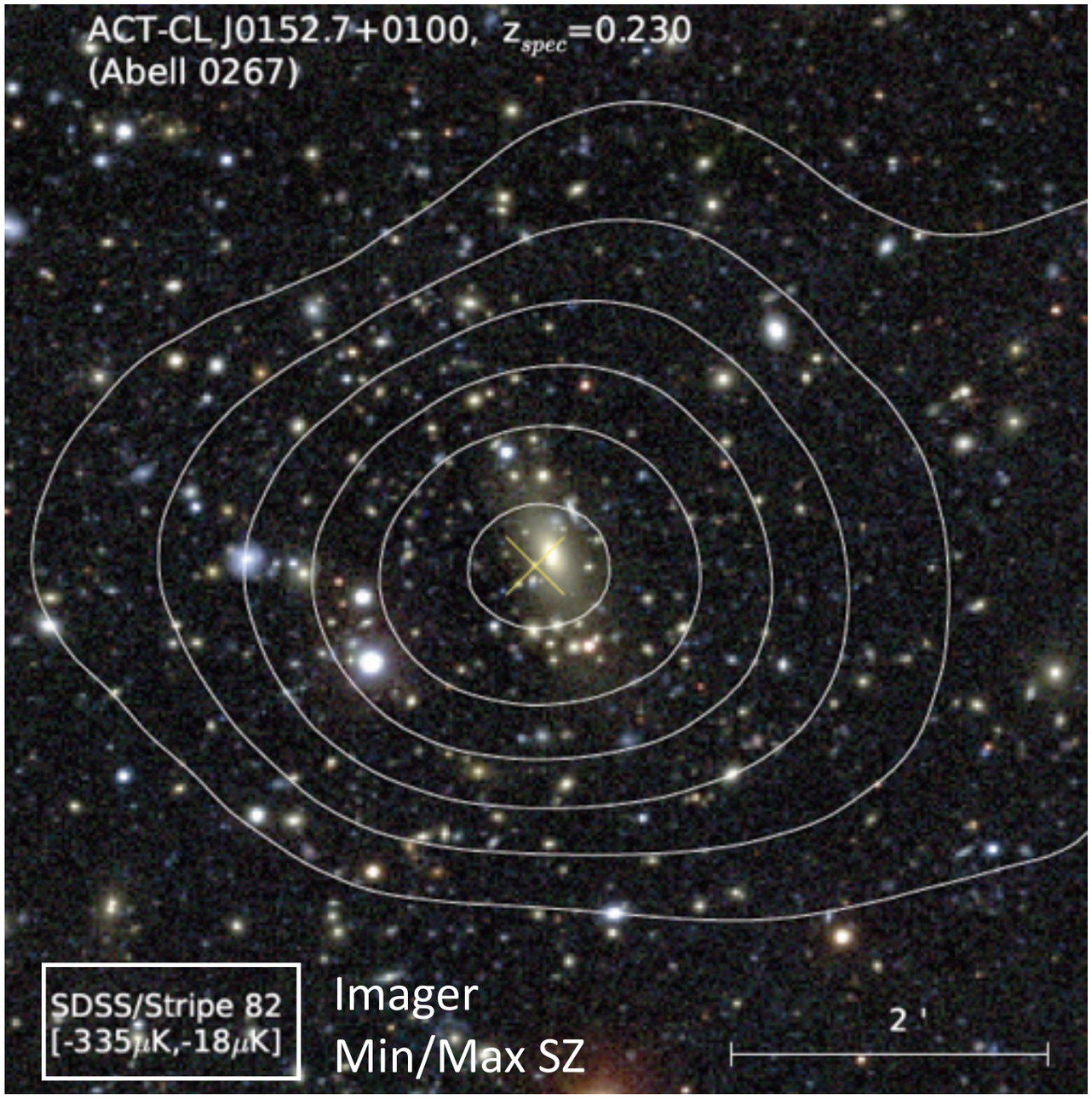

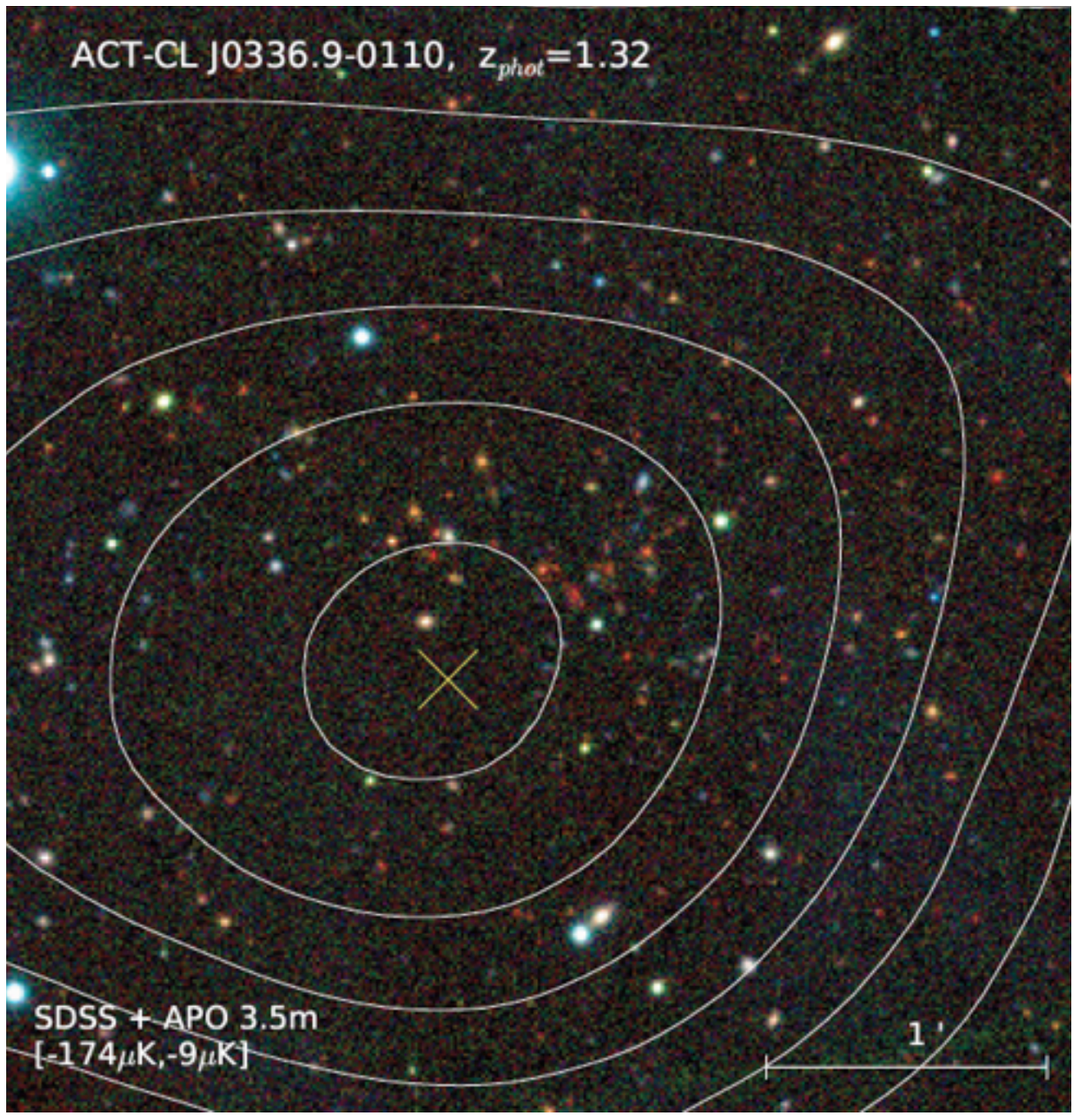

Optical Confirmation

Redshift Measurements (many spectroscopic) and Sample Purity

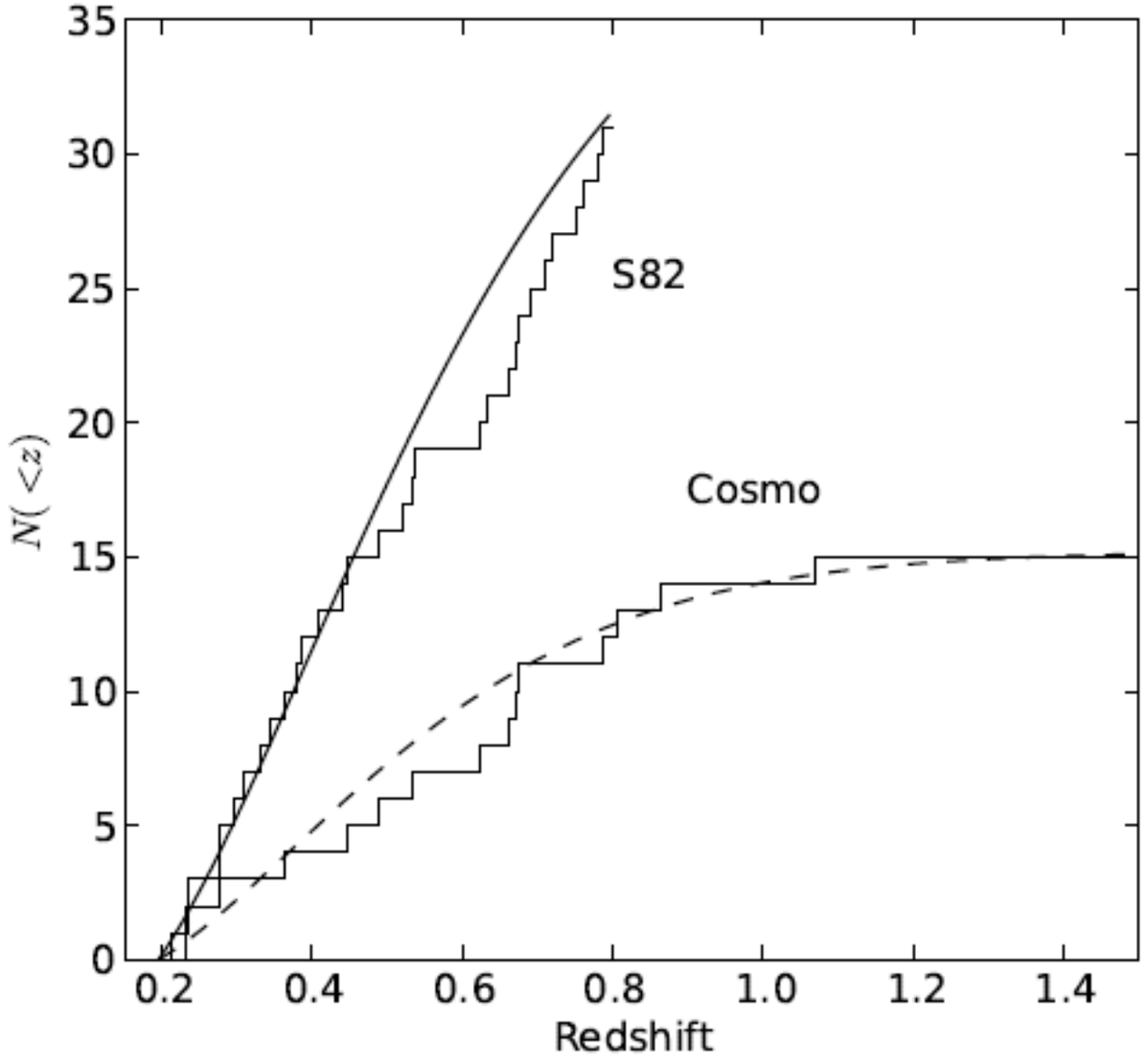

Figure 12. Cumulative number counts for two subsamples of the full cluster catalog for which confirmation is complete. The upper lines are data and model counts for the S82 sample of clusters having $\tilde{y}_0/\delta\tilde{y}_0 > 4$ and $0.2 < z < 0.8$. The lower lines represent the cosmological sample of 15 clusters with fixed-scale $\tilde{y}_0/\delta\tilde{y}_0 > 5.1$ and $z > 0.2$. The model for the counts is obtained from a maximum likelihood fit, with only σ_8 as a free parameter. The model includes a full treatment of selection effects for the sample under consideration.

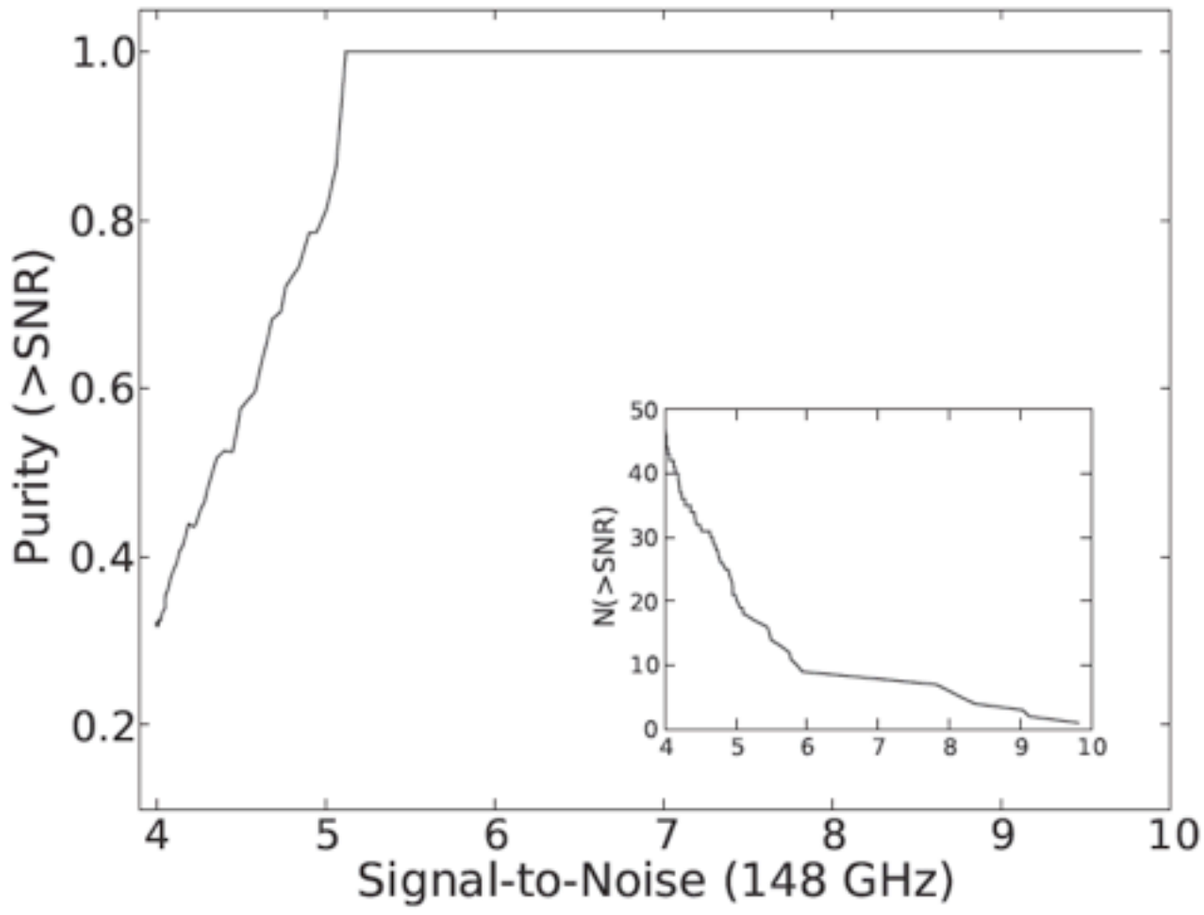

Figure 10. The S82 SZ cluster sample purity greater than a given S/N in the ACT 148 GHz maps. The purity is defined as the ratio of the number of confirmed clusters to the number of observed clusters candidates. The solid line represents the purity binned in $n = 2$ events. The inset plot shows the cluster cumulative distribution as a function of S/N for the optically-confirmed cluster sample.

Optical Confirmation

Redshift Measurements (many spectroscopic) and Sample Purity

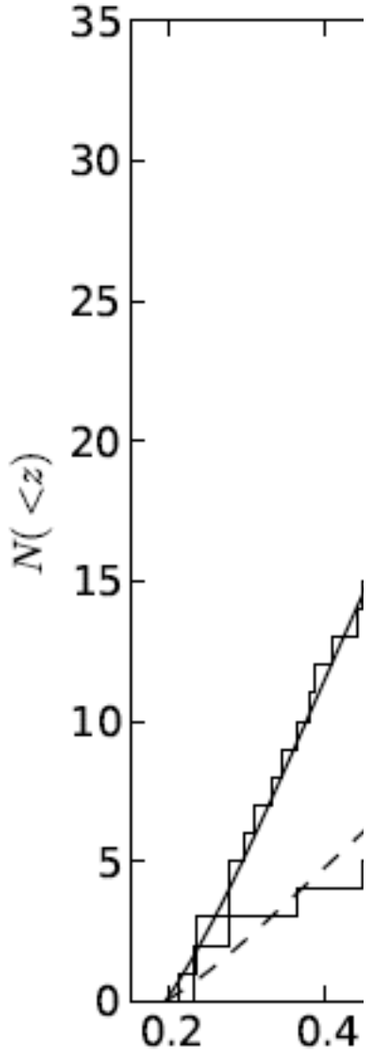

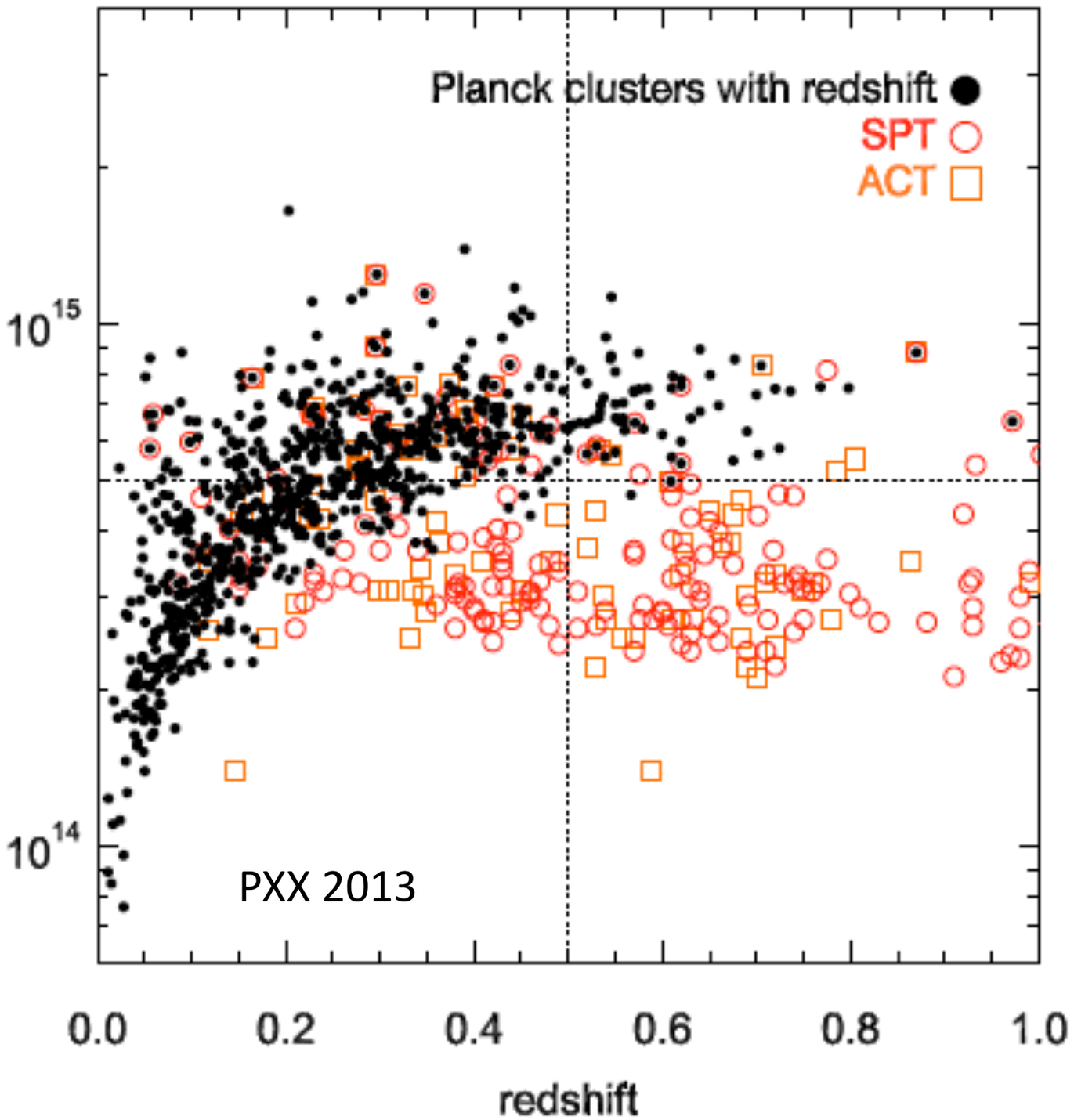

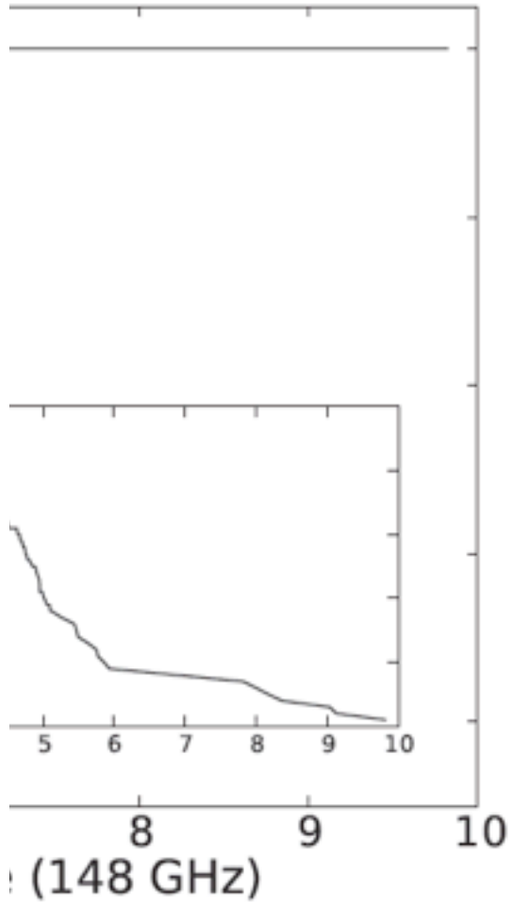

Figure 12. Cumula
full cluster catalog f
lines are data and
having $\widetilde{y}_0/\delta\widetilde{y}_0 > 4$ a
the cosmological sar
5.1 and $z > 0.2$. T
maximum likelihood
model includes a ful
under consideration.

ity greater than a given S/N in the
as the ratio of the number of con-
clusters candidates. The solid line
ts. The inset plot shows the clus-
f S/N for the optically-confirmed

From y_{sz} to Mass

$$\widetilde{y}_0 = 10^{A_0+A} E(z)^2 (M/M_{\rm pivot})^{1+B_0+B} \times$$
$$Q\left[\left(\frac{1+z}{1.5}\right)^{C} \theta_{500}/m^{C_0}\right] f_{\rm rel}(m,z).$$

A = Normalization

B = Mass Scaling

C = Redshift Evolution

(σ = Intrinsic Scatter)

A0, B0, C0 correspond to the Universal Pressure Profile (UPP) based scaling parameters (Arnaud+ 2010), so UPP has A=B=C=0.

SZ-Mass Relation -- Fits to Sims

Fit A (normalization), B (mass power law scaling), C (redshift dependence) & intrinsic scatter to Sims

Three Simulations:

Bode et al 2012

- "B12" (attempt at realistic feedback included)

Trac et al 2012

- Adiabatic (No feedback)
- Nonthermal20 (20% of pressure nonthermal)

Adiabatic will give largest Y for given M

Nonthermal20 the smallest

B12 is in between.

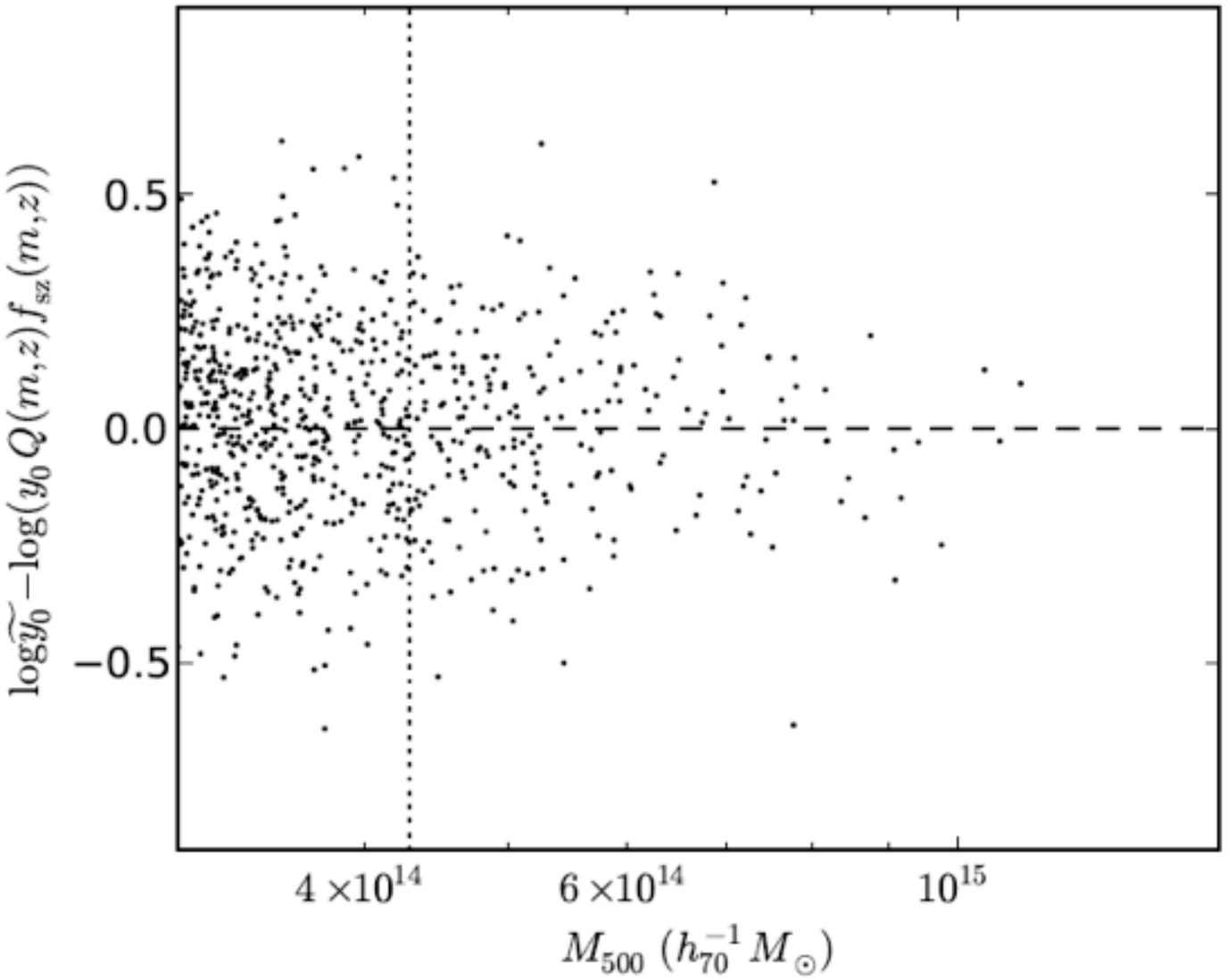

Figure 9. Residuals of the scaling relation fit for the B12 model (Section 3.4). Only clusters with $0.2 < z < 1.4$ and $M_{500c} > 4.3 \times 10^{14}\ h_{70}^{-1}\mathrm{M}_\odot$ (indicated by dotted line) are used for the fit. The scatter in the relation is measured from the RMS of the residuals.

SZ-Mass Relation -- Sim Results

Results from Fits to Sims

Description	A_m	B	C	$\sigma_{\rm int}$
Universal Pressure Profile (UPP)	0	0	0	0.20[a]
Models (§3.4)				
B12	-0.17 ± 0.06	-0.00 ± 0.20	-0.04 ± 0.37	0.20
Nonthermal20	-0.29 ± 0.06	0.00 ± 0.20	0.67 ± 0.47	0.21
Adiabatic	-0.02 ± 0.06	-0.08 ± 0.20	0.10 ± 0.43	0.21

+ As expected Non-thermal processes decrease SZ given a mass
+ Adiabatic equivalent to UPP
+ **For M > 4.3x10^{14} M$_\odot$, The main difference is in the normalization A**

SZ-Mass Relation -- Fit to M_{dyn}

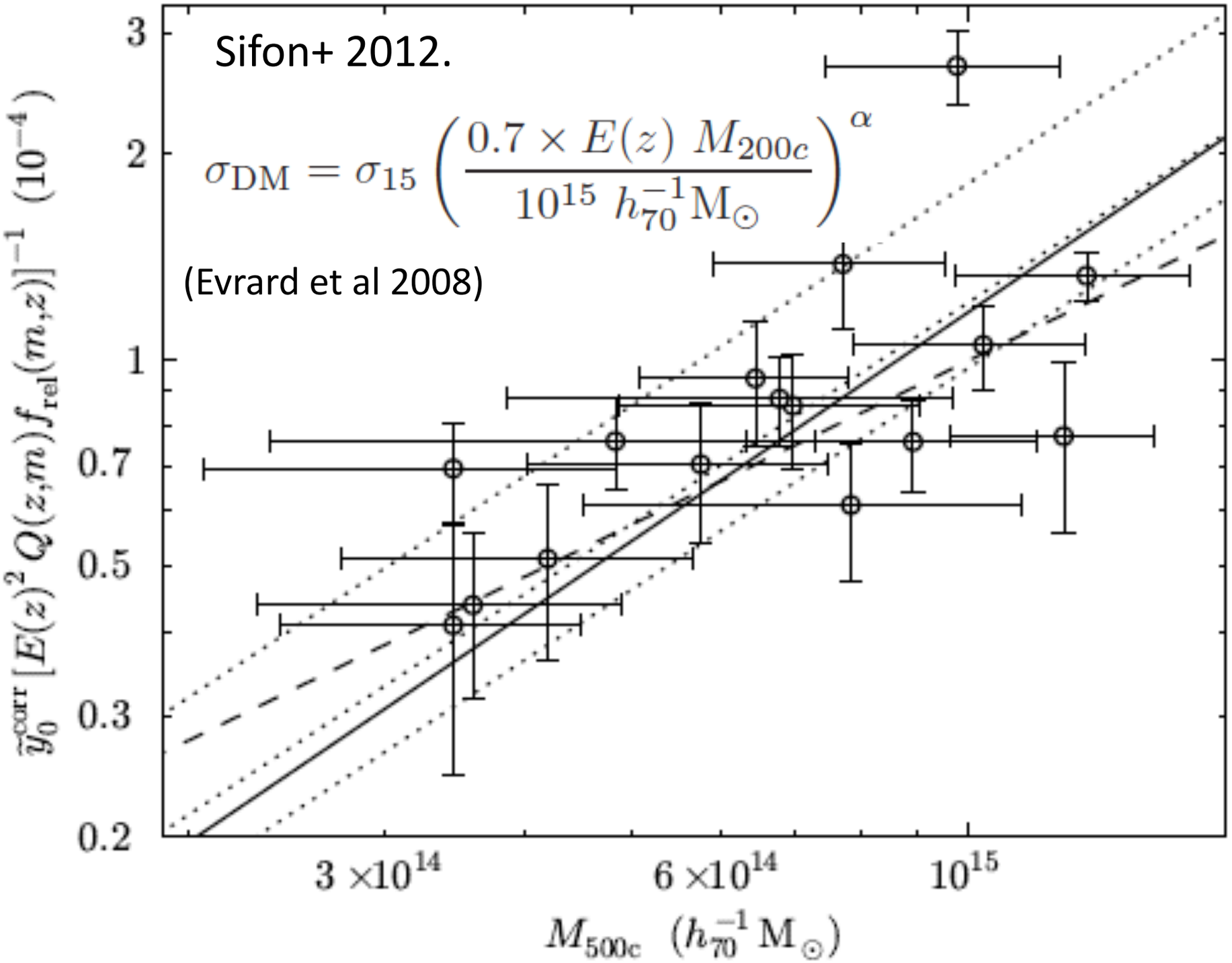

SZ-Mass Relation

Description	A_m	B	C	$\sigma_{\rm int}$
Universal Pressure Profile (UPP)	0	0	0	0.20[a]
Models (§3.4)				
B12	-0.17 ± 0.06	-0.00 ± 0.20	-0.04 ± 0.37	0.20
Nonthermal20	-0.29 ± 0.06	0.00 ± 0.20	0.67 ± 0.47	0.21
Adiabatic	-0.02 ± 0.06	-0.08 ± 0.20	0.10 ± 0.43	0.21
Dynamical mass data (§3.5)				
All clusters	-0.21 ± 0.21	0.03 ± 0.51	0	0.31 ± 0.13
Excluding J0102	-0.11 ± 0.15	-0.28 ± 0.35	0	0.19 ± 0.10

"El Gordo"

Fixed

Dynamical mass results best resemble B12 or Nonthermal (large errors)

Completeness Estimate

Total Sample (S/N>4; solid line):

B12: 90% Complete at **M_{500c}=6x10^{14} M$_\odot$**

UPP: 90% Complete at **4x10^{14} M$_\odot$**

Cosmo Sample (S/N>5.1; dotted line):

B12: 90% Complete at 7x10^{14} M$_\odot$

UPP: 90% Complete at 5x10^{14} M$_\odot$

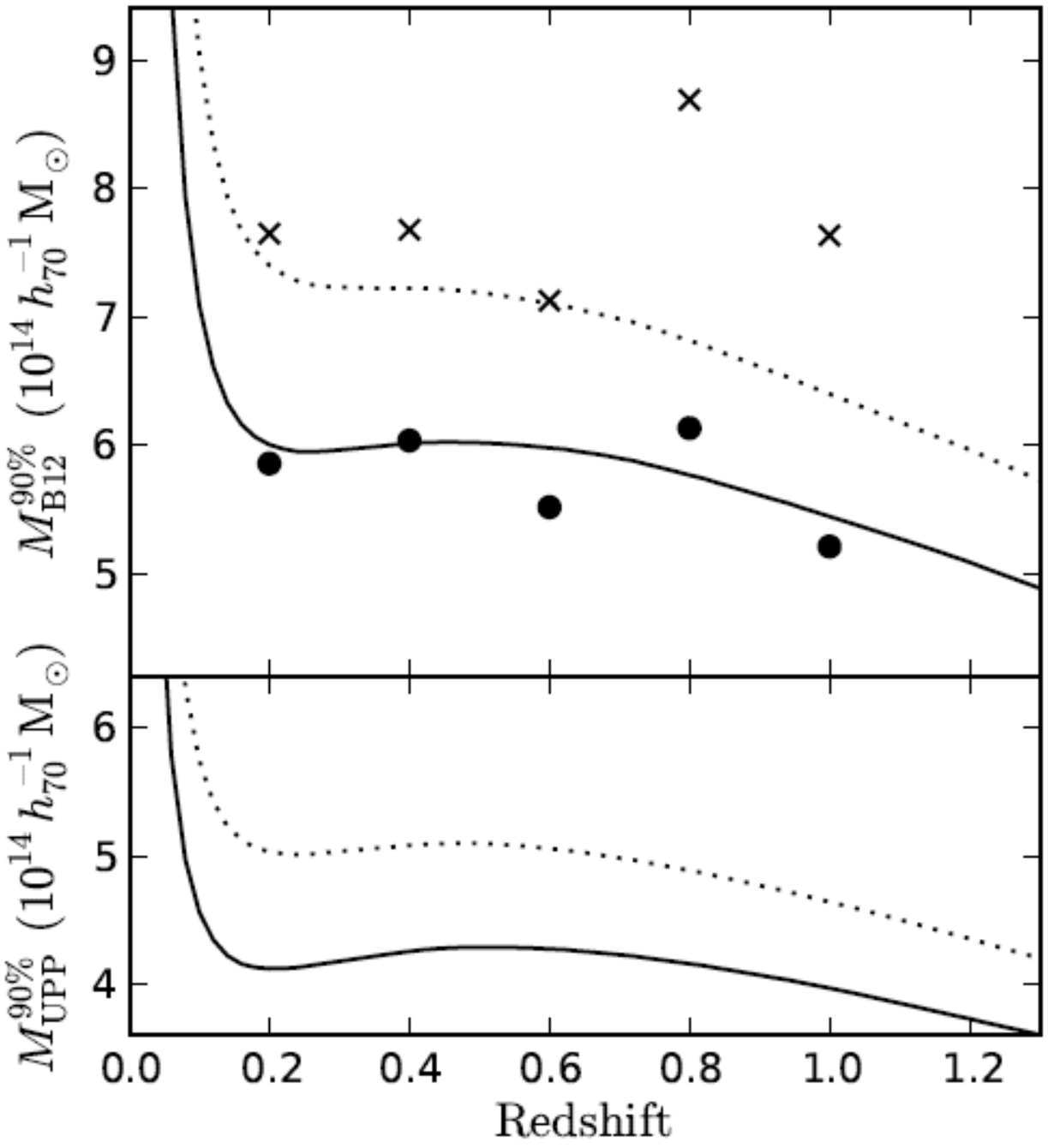

Figure 11. Estimate of the mass (M_{500c}) above which the ACT cluster sample within S82 is 90% complete (see Section 3.6). Lower panel assumes a UPP-based scaling relation with 20% intrinsic scatter; solid line is for $S/N > 4$ (full S82 sample, valid to $z < 0.8$), dotted line is for the $S/N > 5.1$ subsample (valid to $z \approx 1.4$). The upper panel shows analogous limits, but assuming scaling relation parameters obtained for the B12 model (Section 3.4). Circles (crosses) are based on filtering and analysis of B12 model clusters for the $S/N > 4$ (5.1) cut. The completeness threshold decreases steadily above $z \approx 0.6$ because clusters at this mass are easily resolved and the total SZ signal, at constant mass, increases with

Cosmology

15 equatorial clusters with S/N>5.1; 0.2<z<1.4

Fix scaling relation parameters to values from previous fits

Result:

Depending on scaling relation,we can accommodate a broad parameter space.

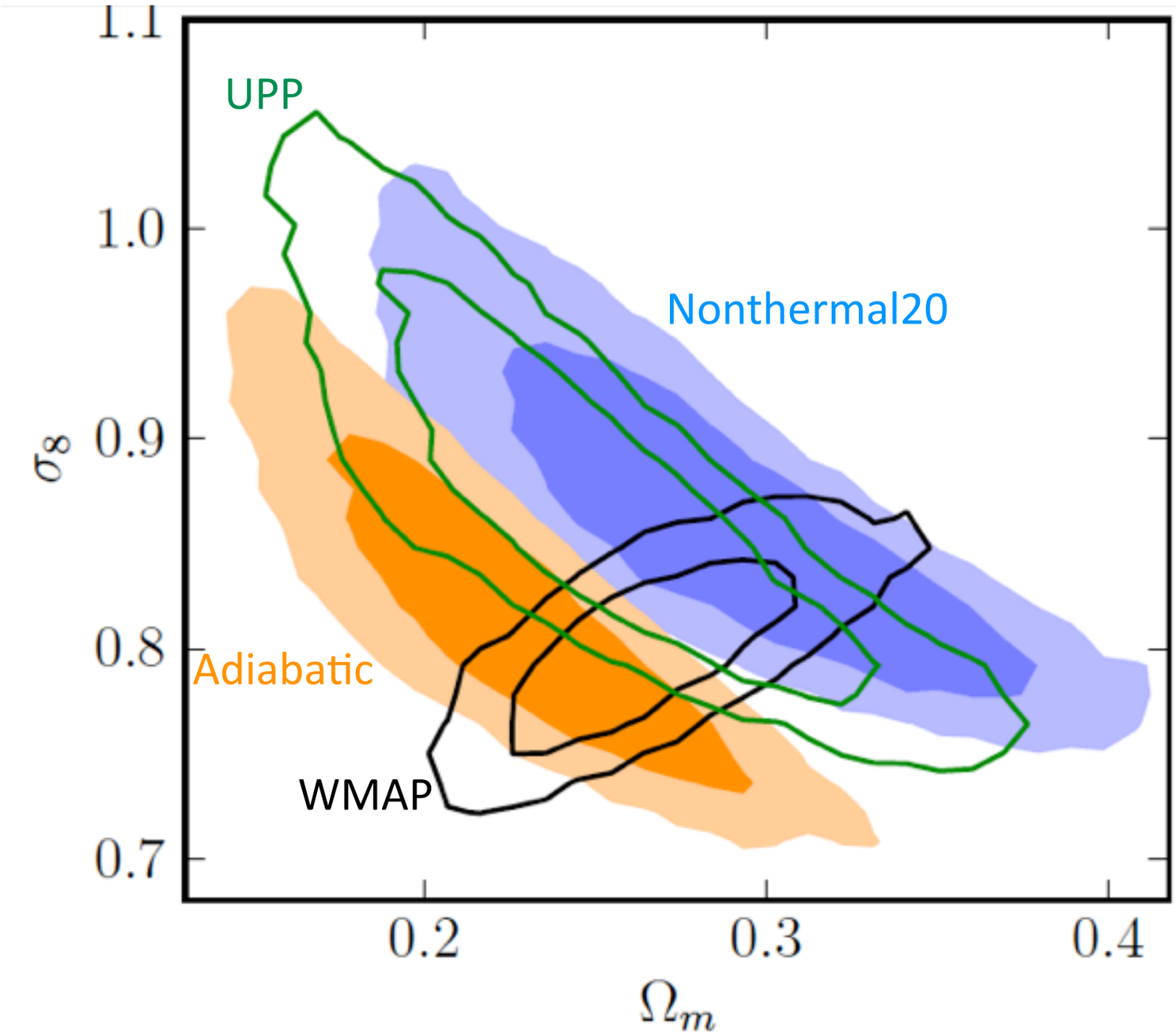

Figure 14. Constraints on ΛCDM cosmological parameters from WMAP7 (black line contours) and ACTcl+BBN+H0 (without CMB information). Contours indicate 68 and 95% confidence regions. ACT results are shown for three scaling relations: UPP (orange contours), B12 (green lines), Nonthermal20 (violet contours). While any one scaling relation provides an interesting complement to CMB information, the results from the three different scaling relations span the range of parameter values allowed by WMAP measurements.

Cosmology

15 equatorial clusters with S/N>5.1; 0.2<z<1.4

+ 7 southern clusters with S/N>5.7; 0.314<z<1.4; and measured m_{dyn}

Marginalize over cosmo and scaling relations, including 15% bias in dynamical mass.

Result:
Constraints favoring high σ_8 likely because of an exceptional sample (El Gordo, Bullet...) but still consistent with other observations.

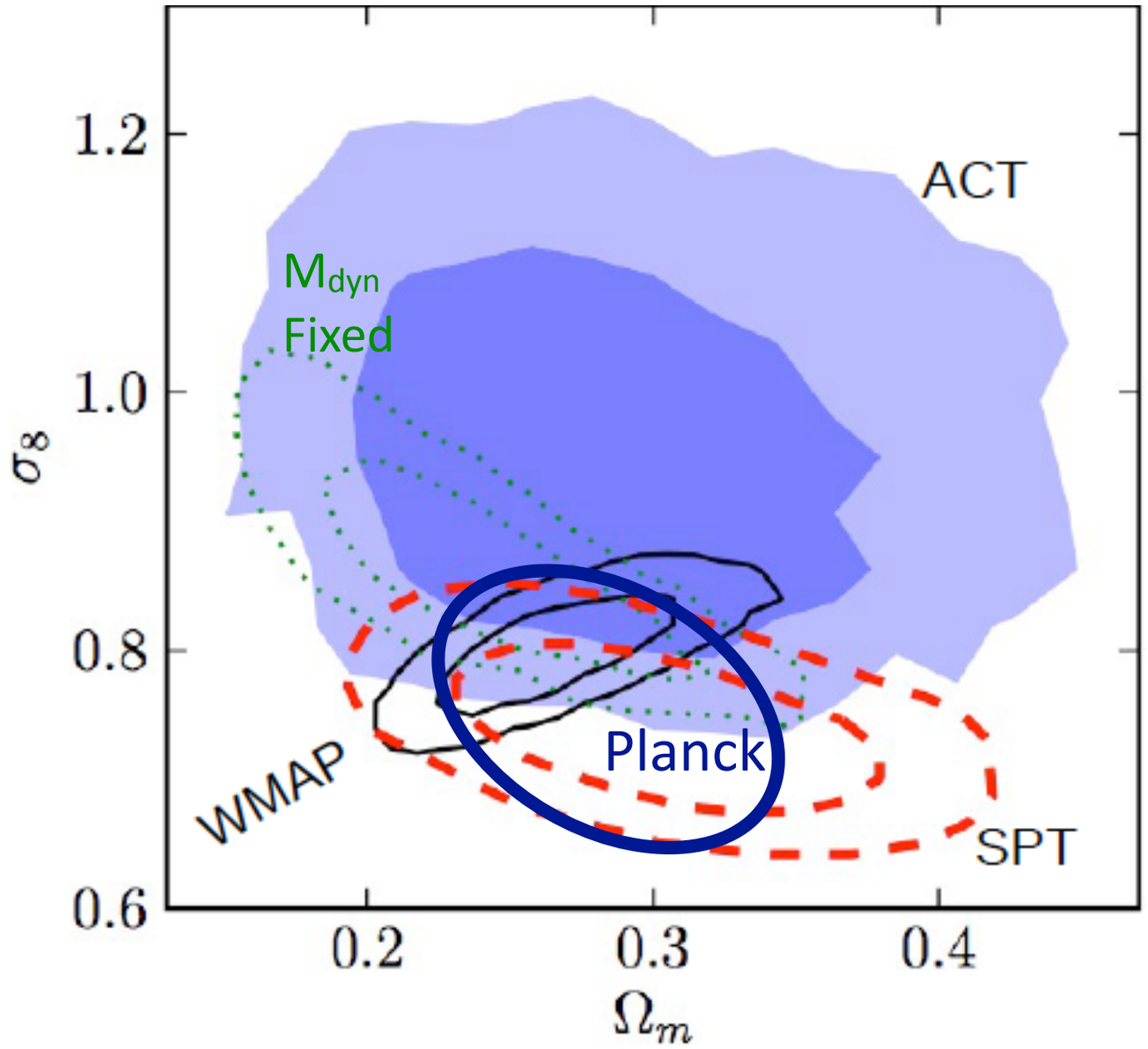

Cartoon of Planck bias marginalized result

Planck: 189 Clusters, 71 with Y_x (PXX 2013)

SPT: 100 Clusters, 14 with Y_x (Benson+2012, Reichardt+2013)

ACT: 22 Clusters, 7 with M_{dyn} (This work)

Next Steps: More Data

(Some Examples)

+ Dynamical data for equatorial sample in hand (Sifon et al 2013, in prep) to obtain more dynamical masses for the “Cosmo” Sample.

+ Chandra data reduced for approximately half the “Cosmological Sample” of 22 clusters, and we have applied for the remaining observations. (Hughes et al 2013, in prep)

+ Sunyaev-Zel’dovich Array follow-up at 30 GHz and higher resolution to obtain complementary SZ data. (Reese et al 2013, in prep)

+ Subaru weak lensing observations of equatorial sample soon (HSC survey)

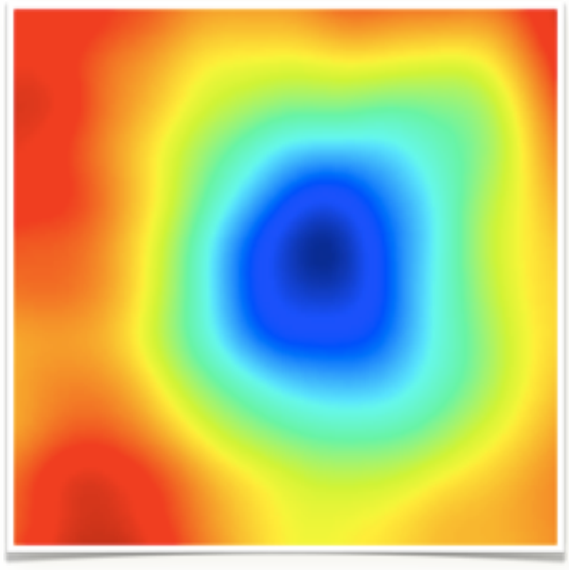

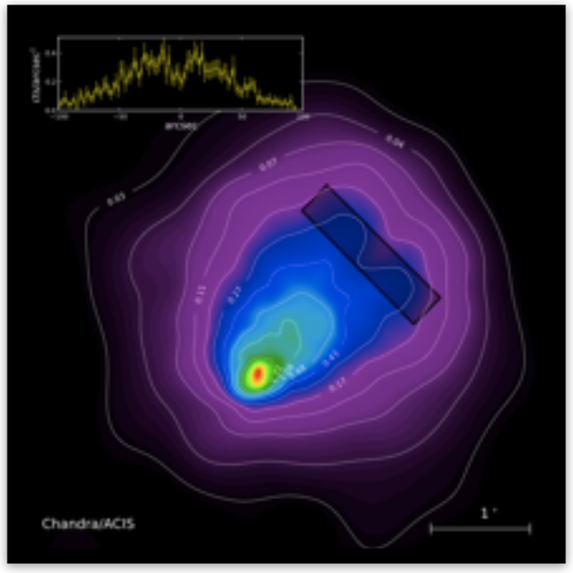

ACT+Chandra for “El Gordo” z=0.87 (ACT-CL J0102-4915)

Awarded Chandra+HST time for full study (Menanteau et al, in prep)

Next Steps: More Data

(Some Examples)

+ Dynamical data for equatorial sample in hand (Sifon et al 2013, in prep) to obtain more dynamical masses for the “Cosmo” Sample.

+ Chandra data reduced for approximately half the “Cosmological Sample” of 22 clusters, and we have applied for the remaining observations. (Hughes et al 2013, in prep)

+ Sunyaev-Zel’dovich Array follow-up at 30 GHz and higher resolution to obtain complementary SZ data. (Reese et al 2013, in prep)

+ Subaru weak lensing observations of equatorial sample soon (HSC survey)

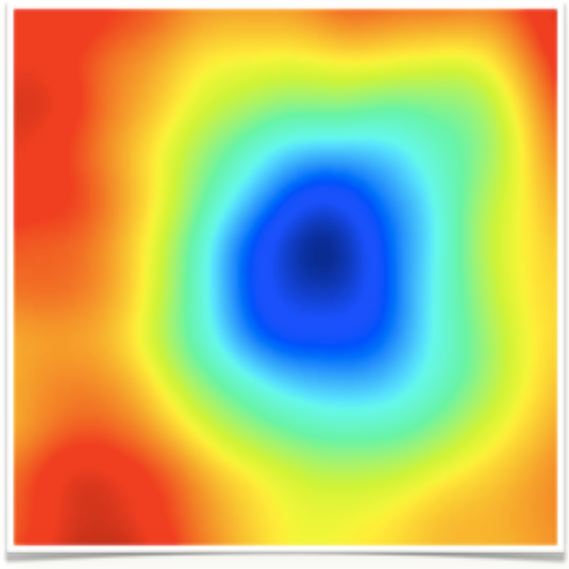

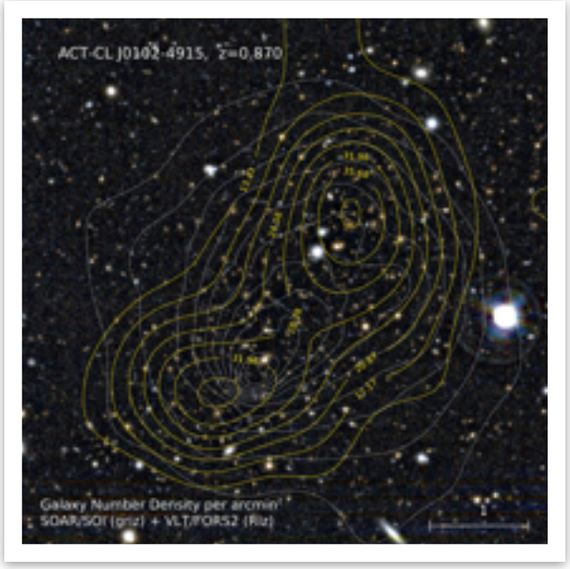

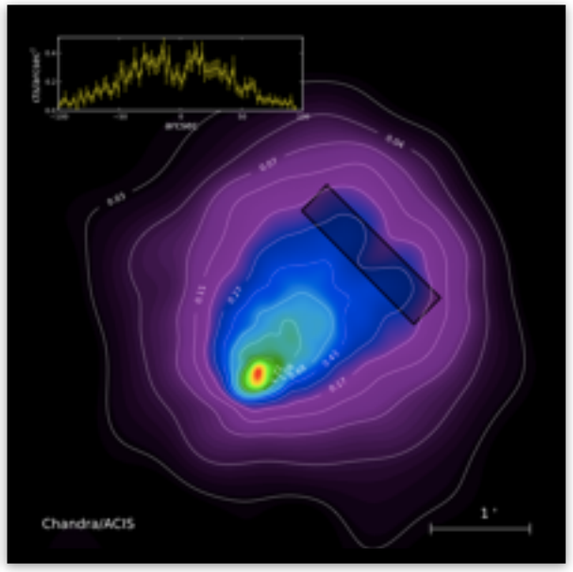

ACT+Chandra for “El Gordo” z=0.87 (ACT-CL J0102-4915)

Awarded Chandra+HST time for full study (Menanteau et al, in prep)

Working To Constrain Inner and Outer Scales with SZA/CARMA+ACT+Planck

More SZA data on all S/N>6 Equatorial Clusters Reese et al 2013, in prep

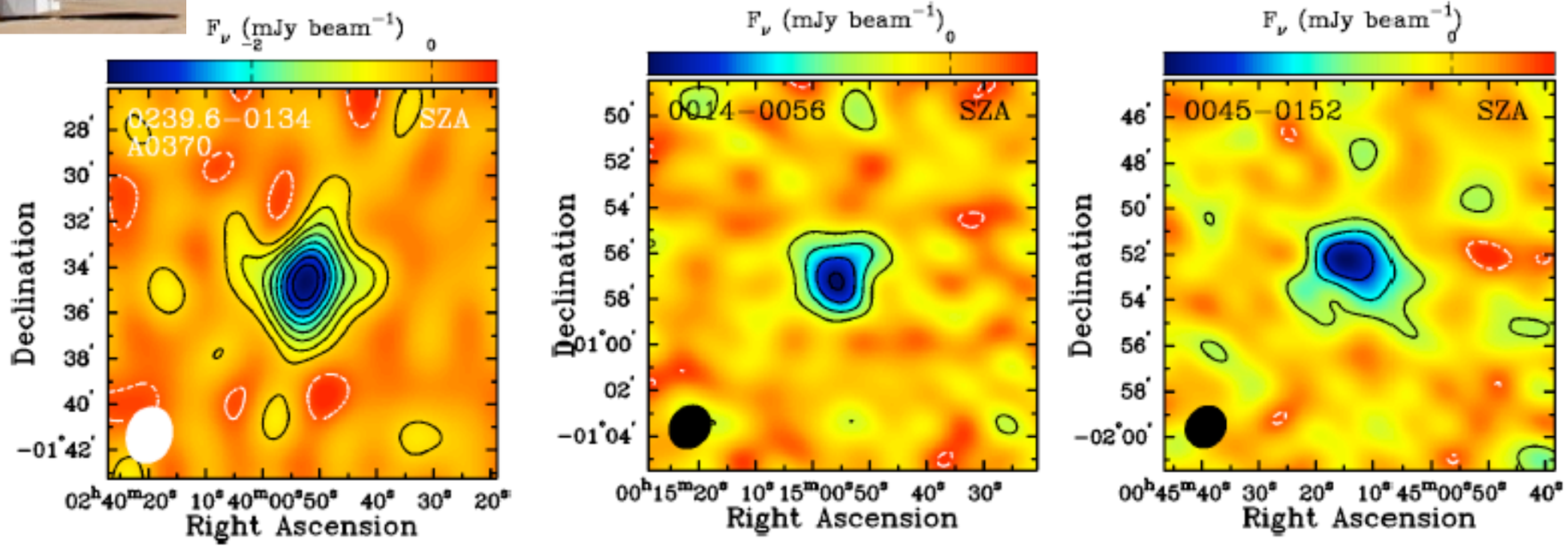

First robust detection of KSZ (from ACT) associated with pairwise galaxy velocities (from BOSS).

Hand+ 2012

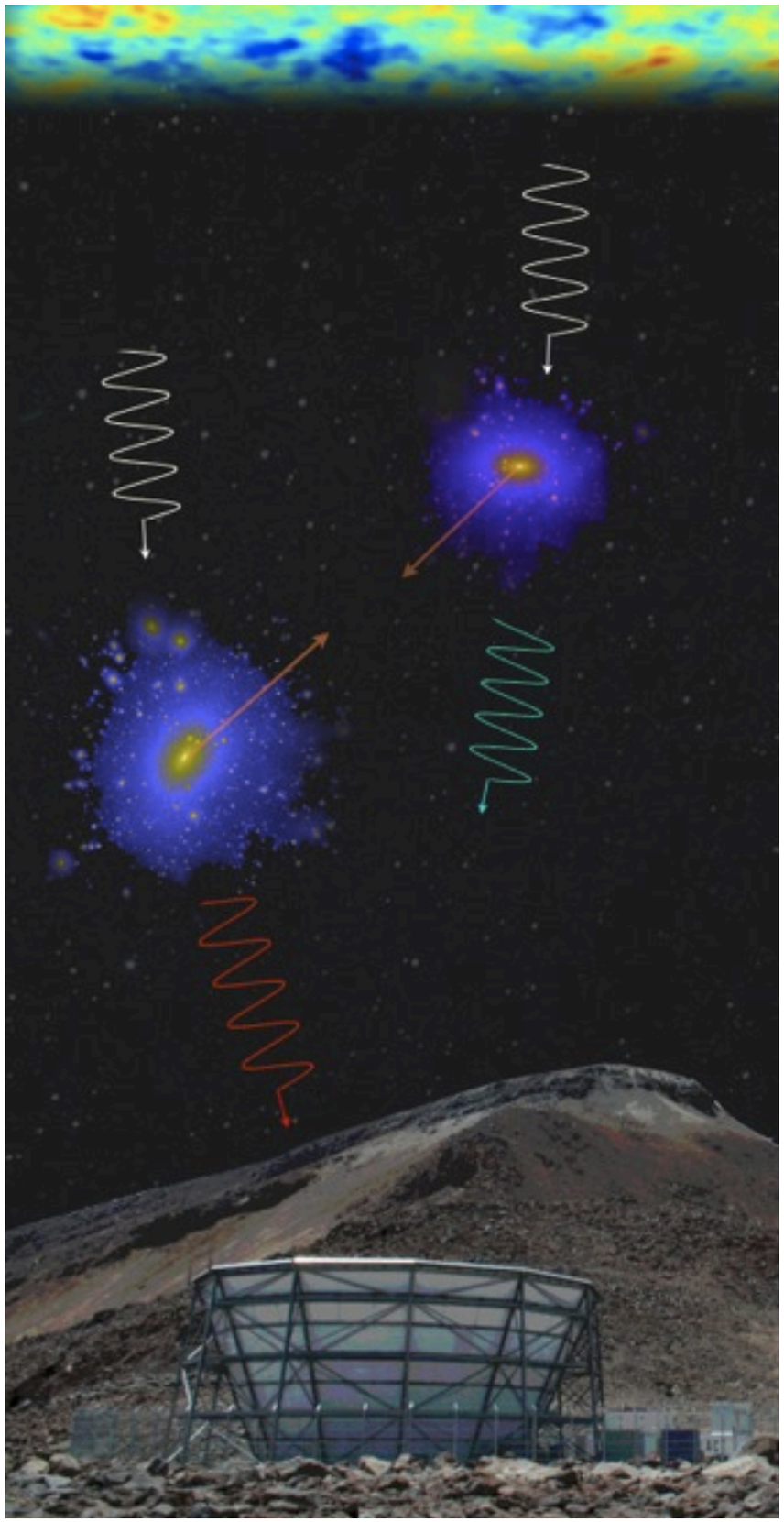

Probing linear velocity field

$$\tilde{p}_{\rm kSZ}(r) = -\frac{\sum_{i<j}\left[(T_i - \mathcal{T}(z_i)) - (T_j - \mathcal{T}(z_j))\right] c_{ij}}{\sum_{i<j} c_{ij}^2}.$$

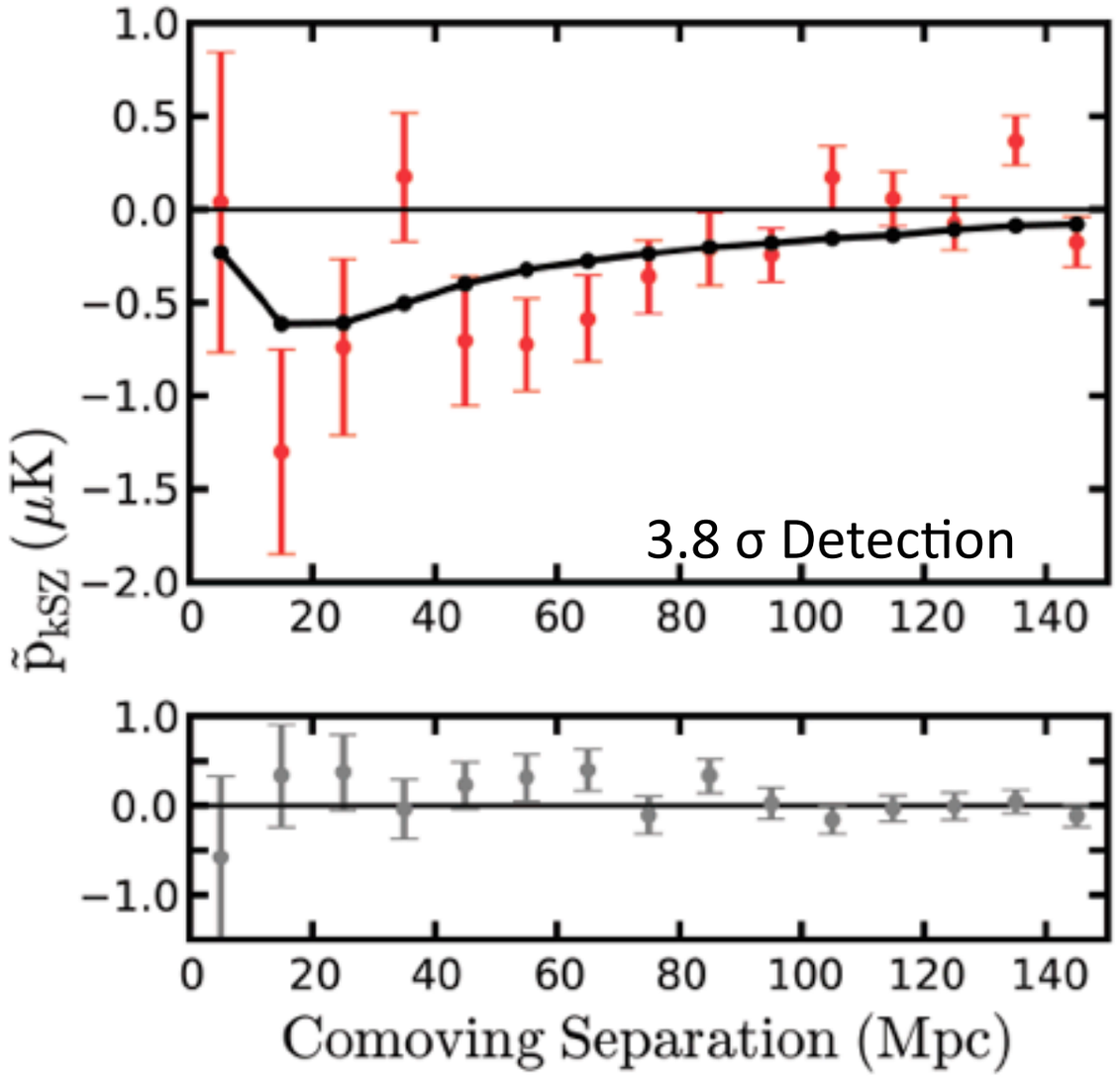

Amplitude consistent with standard structure formation scenario.

New ACT Survey: ACTPol

Same Telescope New Receiver

- Deployed to Atacama January 2013
- Much More Sensitive than first receiver
- 4000 sq-deg medium (20 uK-arcmin) survey
- 150 sq-deg deep (4 uK-armin) survey
- Equatorial Latitudes
- ~1000 Clusters Expected

M. Niemack et al. (2010), 1006.5049

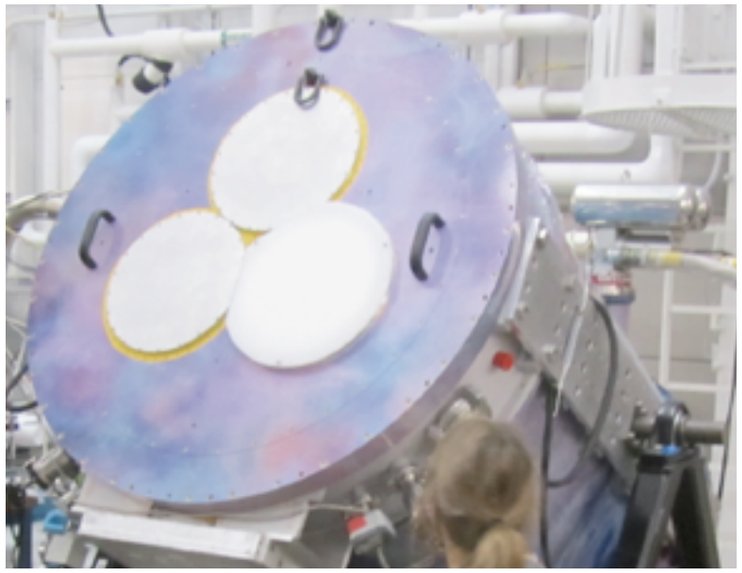

Overlap with many multifrequency datasets, including Subaru Hyper Suprime Cam (HSC) lensing survey and Prime Focus Spectrograph (PFS) survey. (Think Sloan photometry/spectroscopy with Subaru instead of the APO 2.5 meter.)

Next-Next Generation: **Advanced ACTPol**

65% of the sky from 30-300 GHz.

~16,000 polarization sensitive multichroic detectors

Advanced ACTPol
Sky Coverage

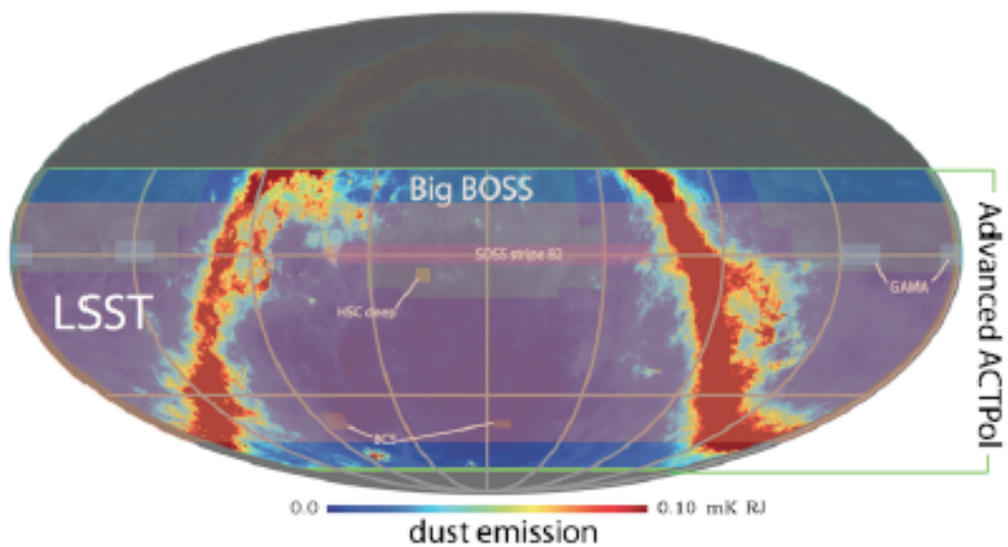

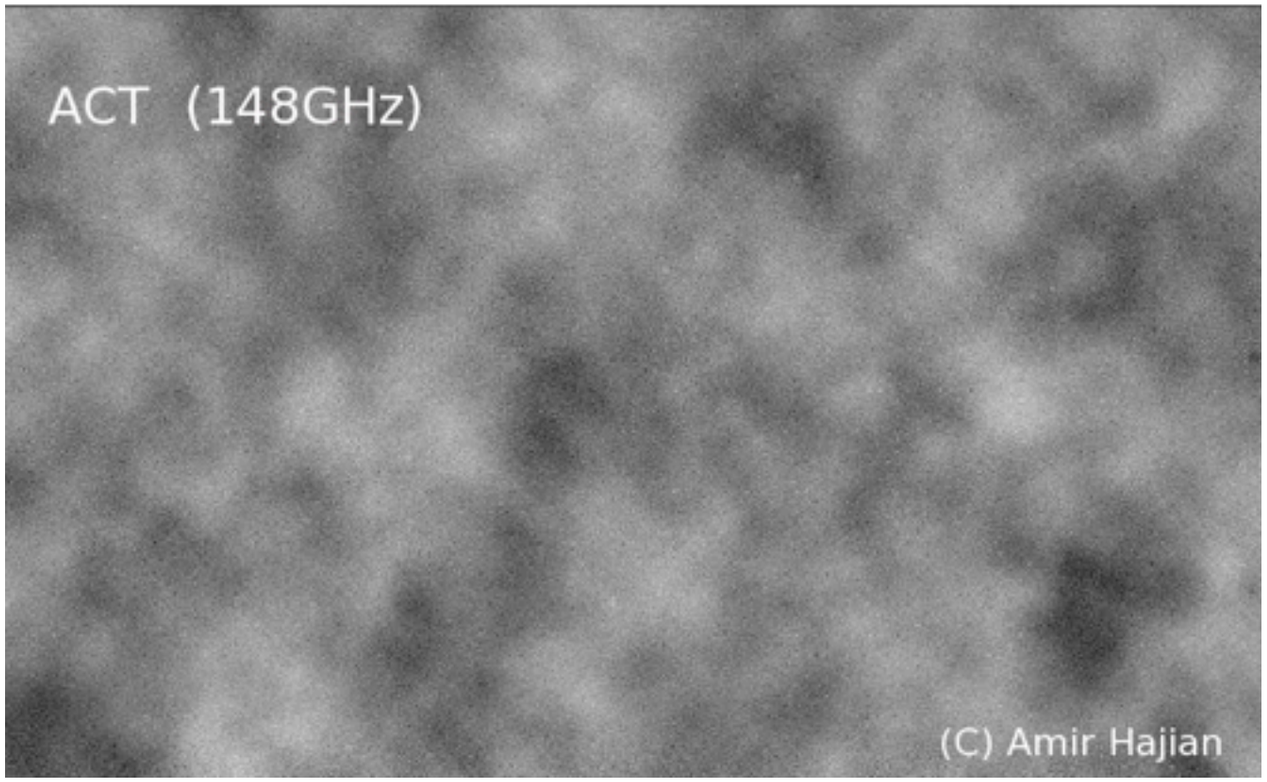

Einde

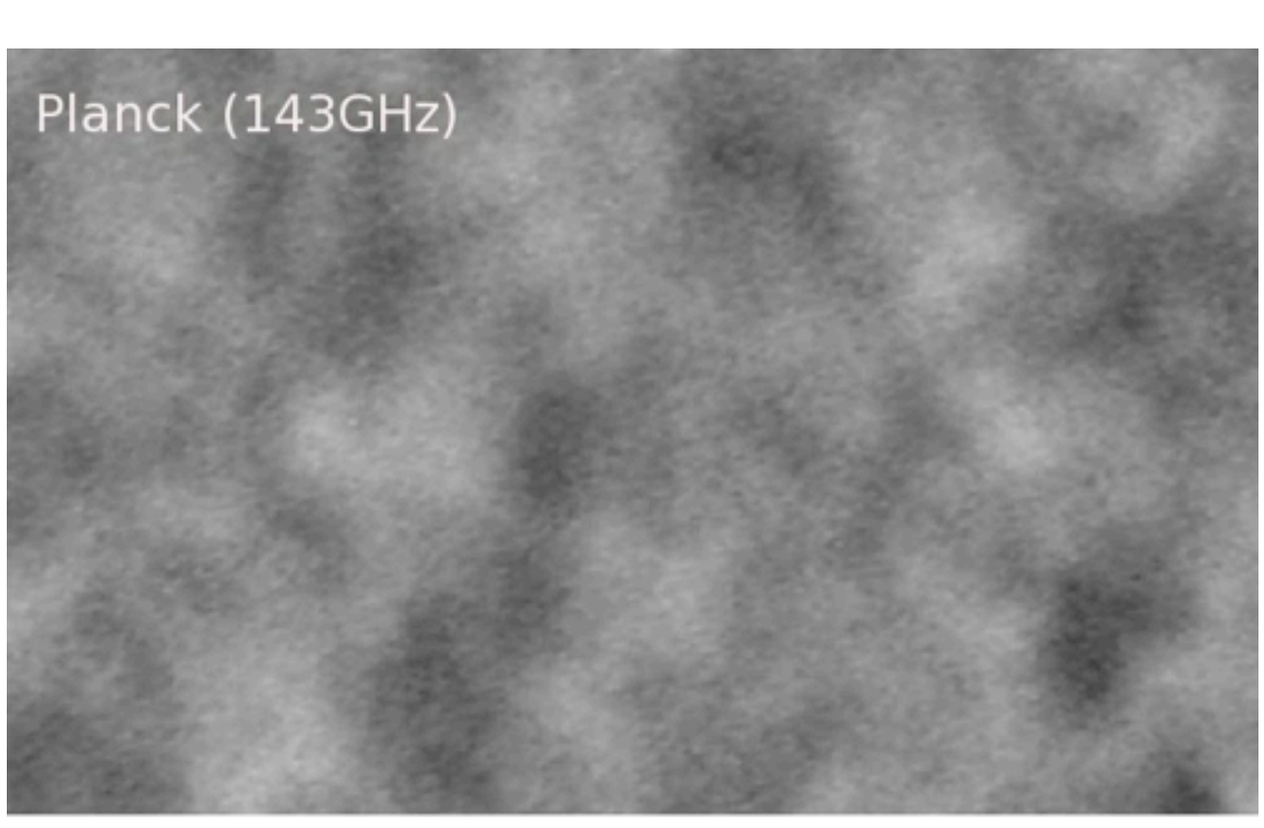

Auxilliary

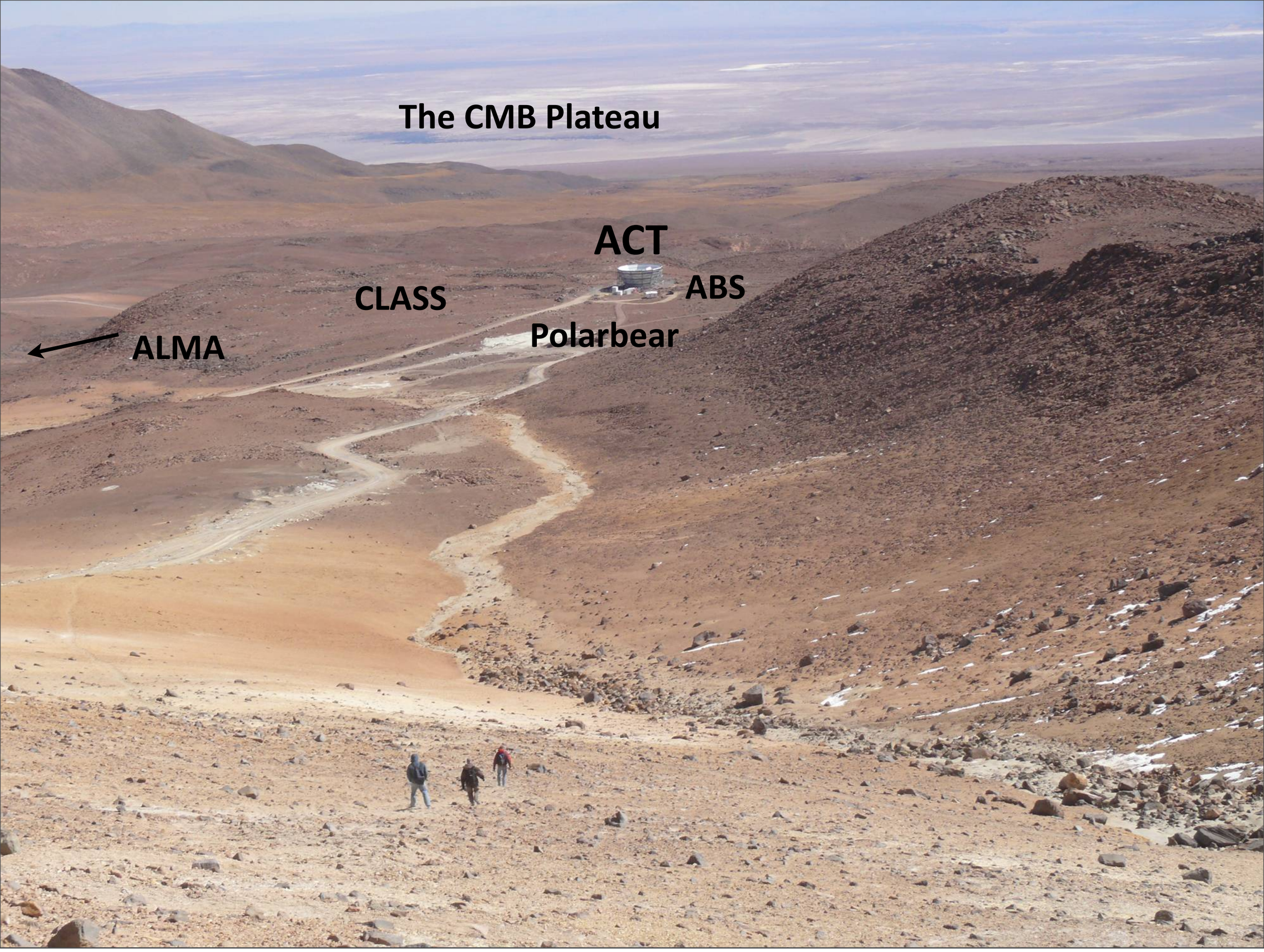
The CMB Plateau
ACT
ABS
CLASS
Polarbear
ALMA

ACT Maps

Dünner et al 2013

Signal Recovery from Acoustic Oscillation to Cluster Scales

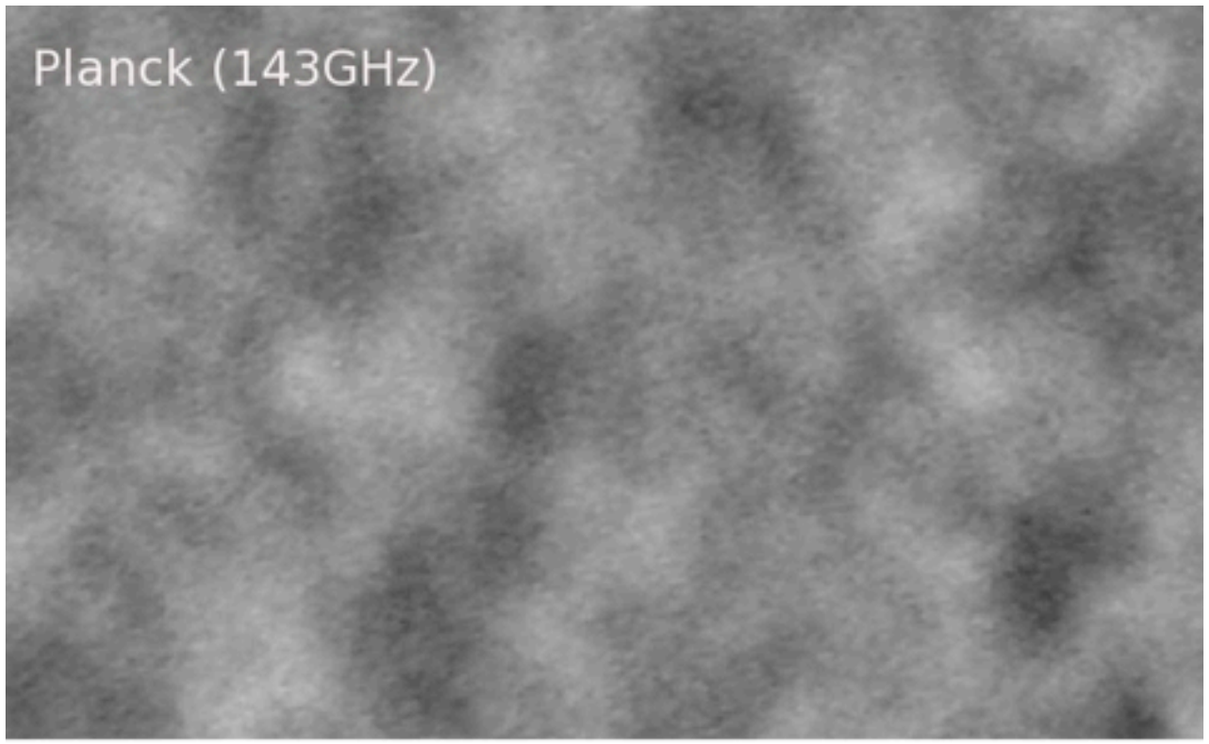

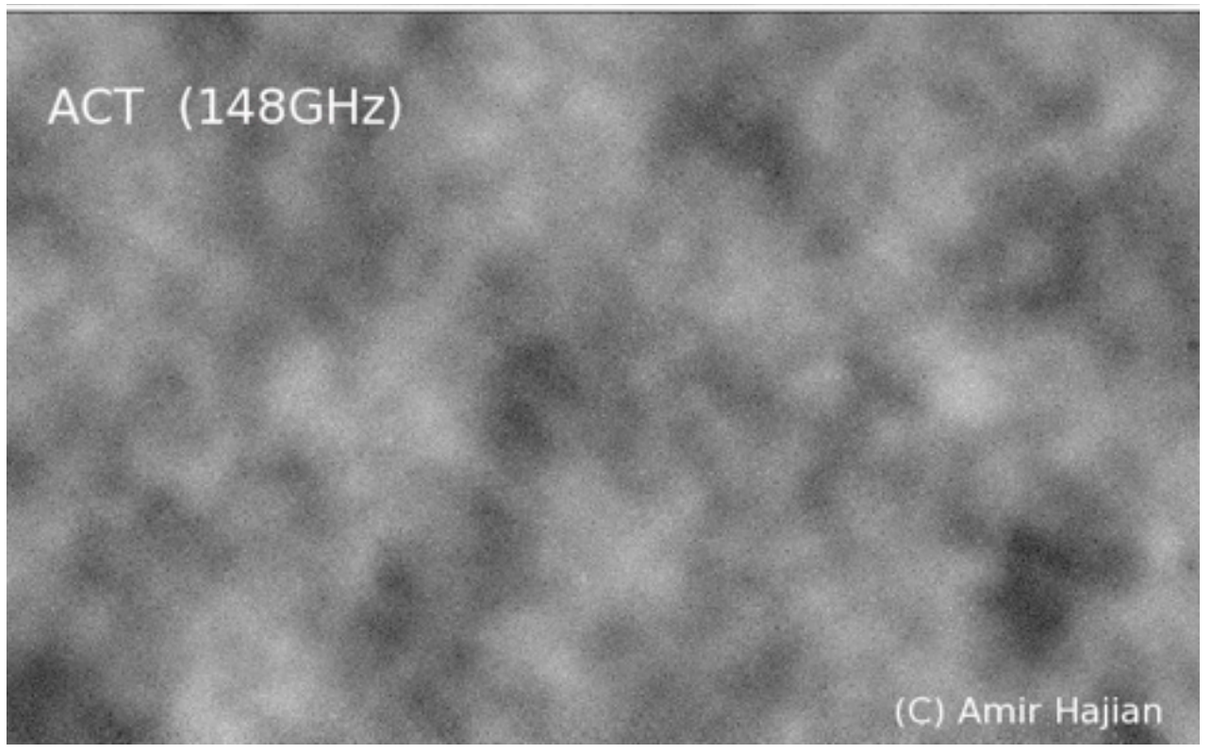

148 GHz, 218 GHz
reduced so far;
277 GHz is almost
there

ACT Maps

Dünner et al 2013

Signal Recovery from Acoustic Oscillation to Cluster Scales

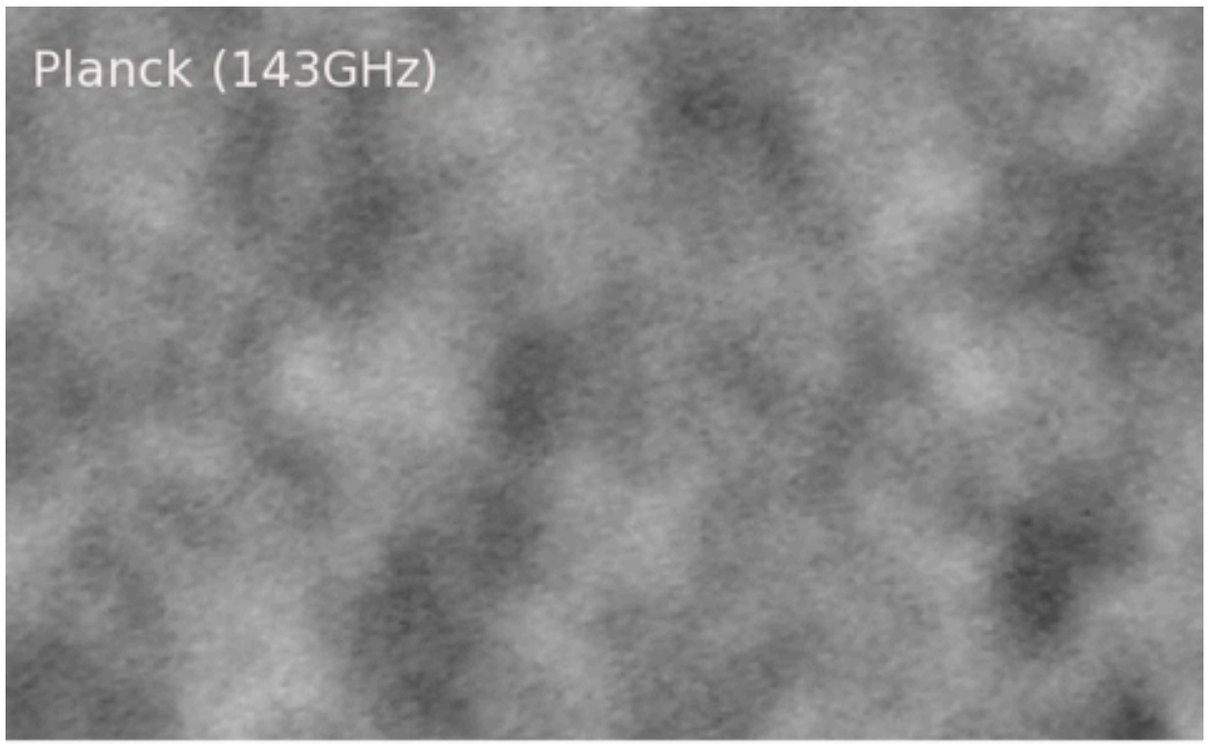

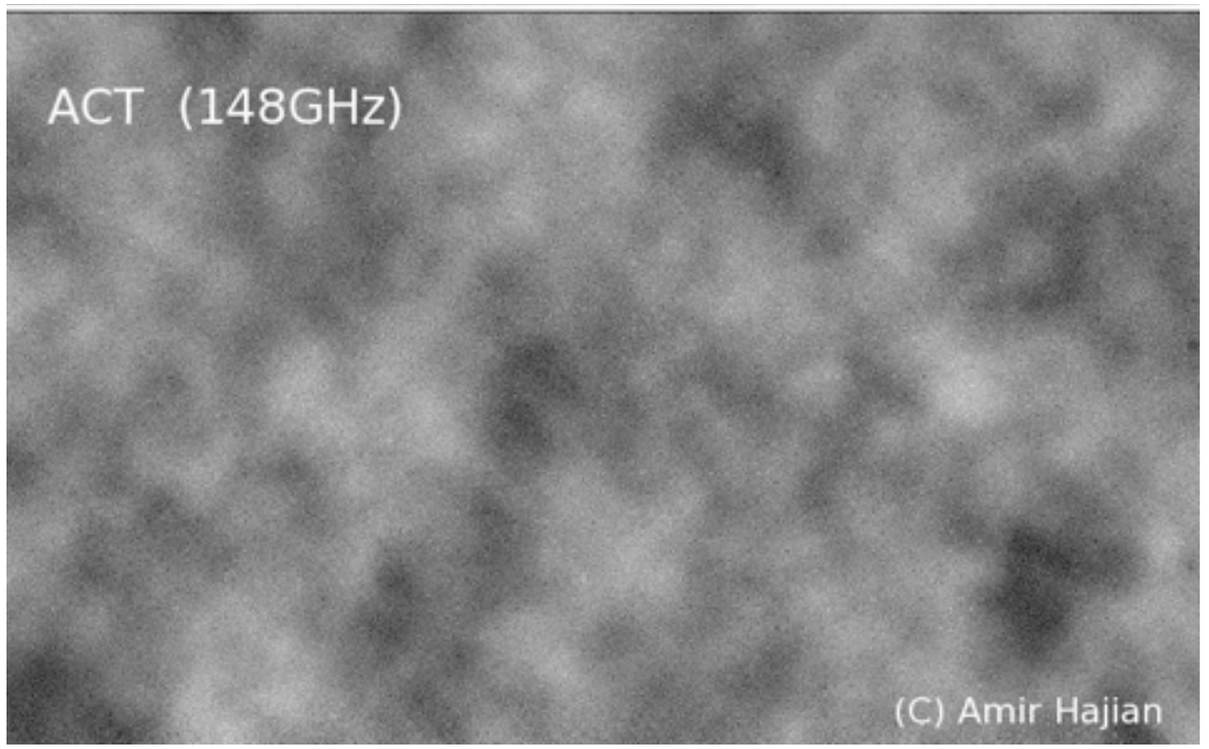

148 GHz, 218 GHz reduced so far; 277 GHz is almost there

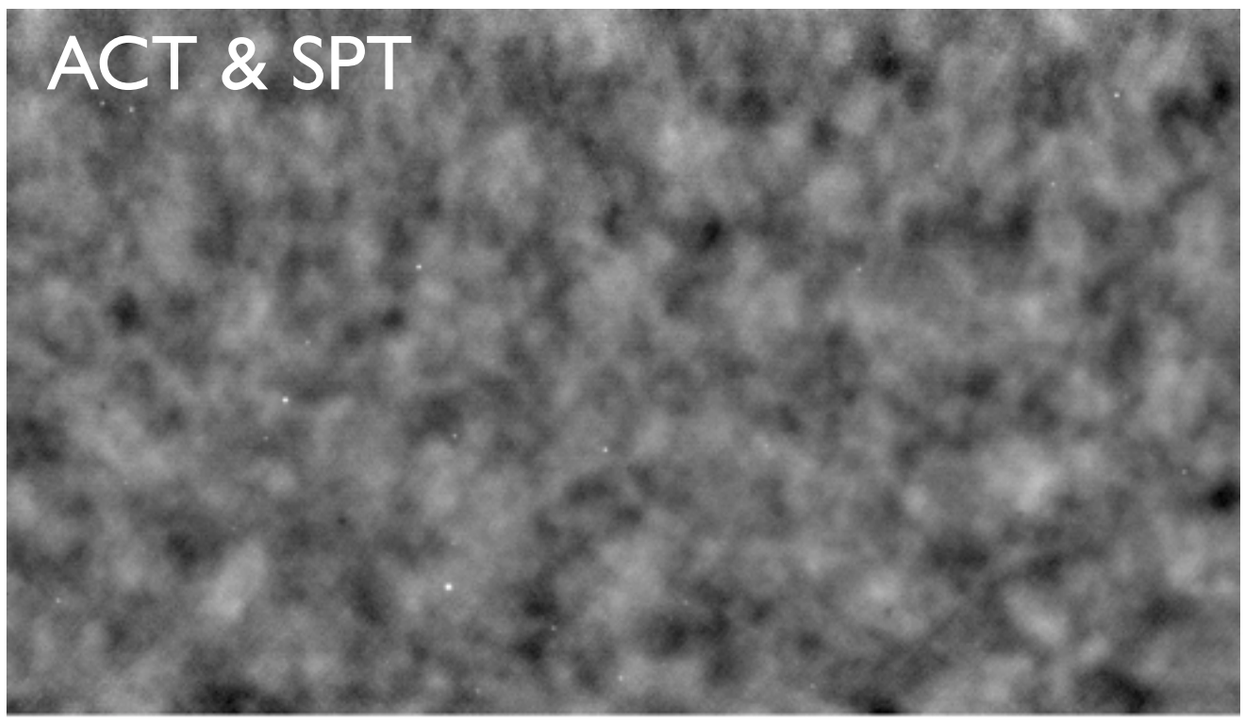

ACT ell > 300

ACT Angular Power Spectrum

Das+2013, Dunkley+2013

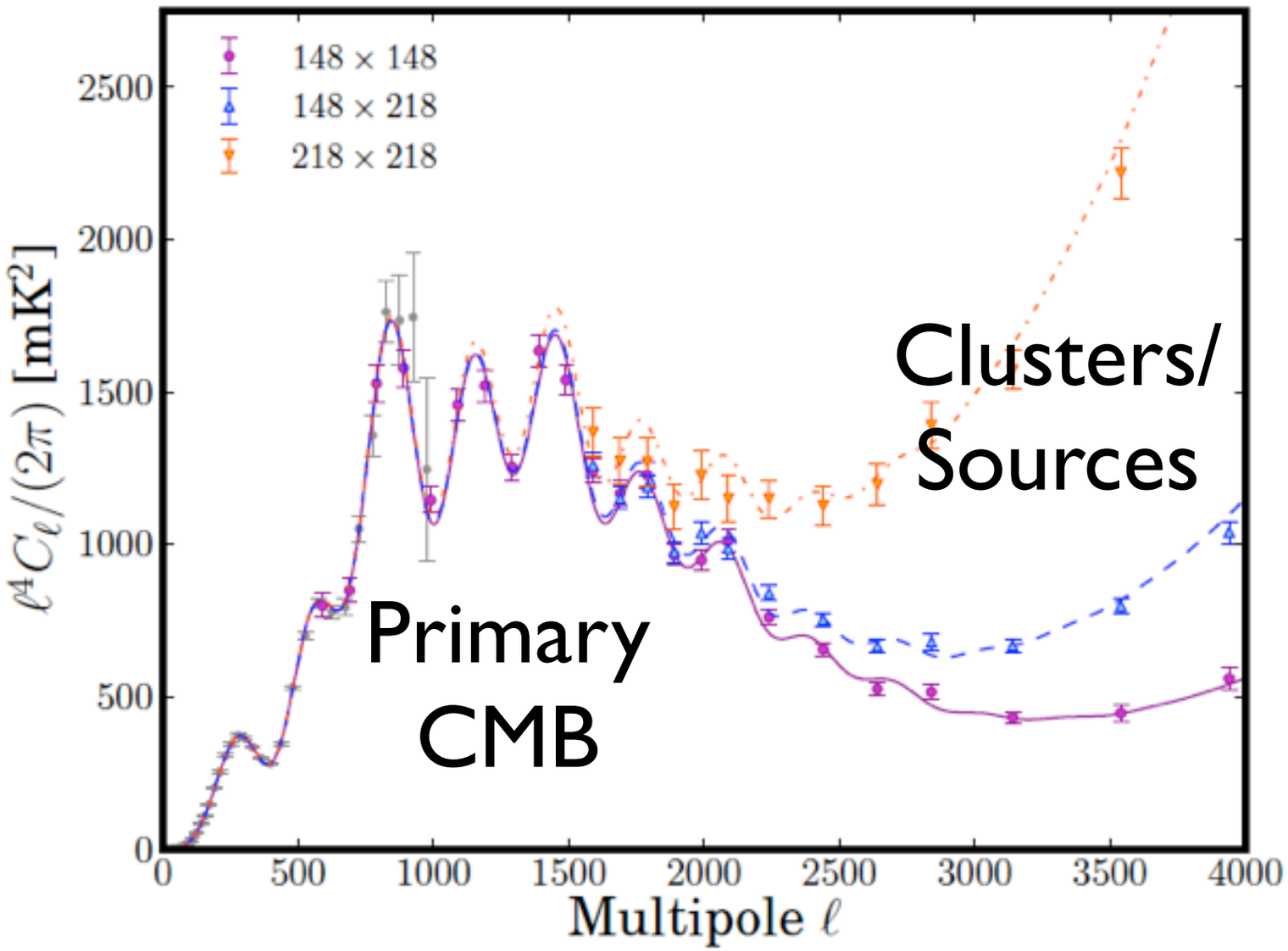

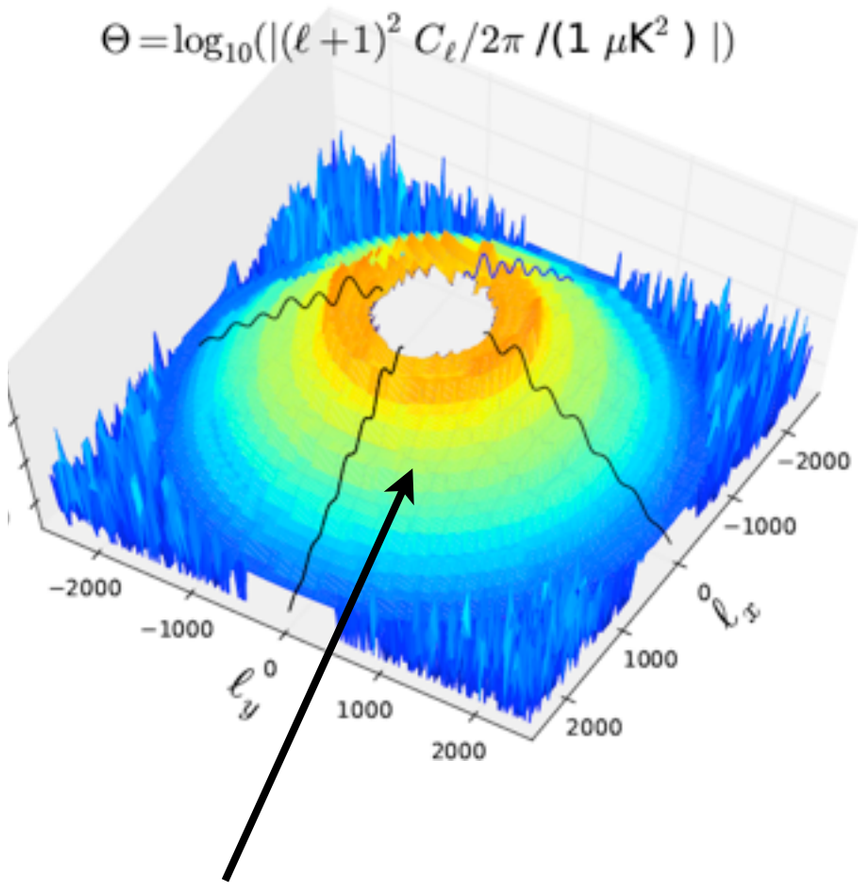

Sample Variance Limited

Das, Louis, Nolta et al

Cluster Extraction Harmonic View

Matched filter acts as band pass filter, removing CMB at low angular frequencies and smoothing over noise at high angular frequency.

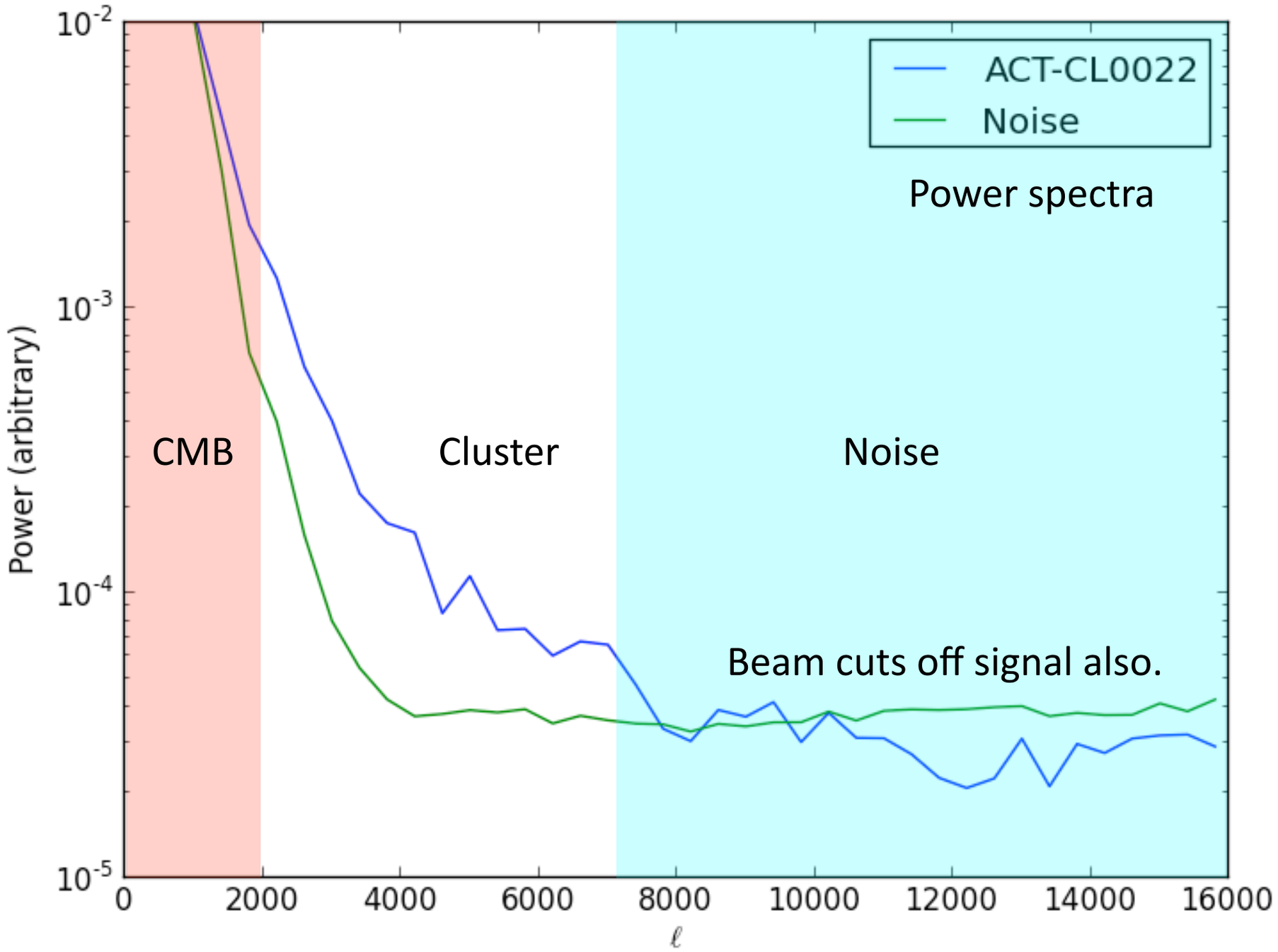

Catalog Results

Ten Most Significant Decrements (Filtered Map)

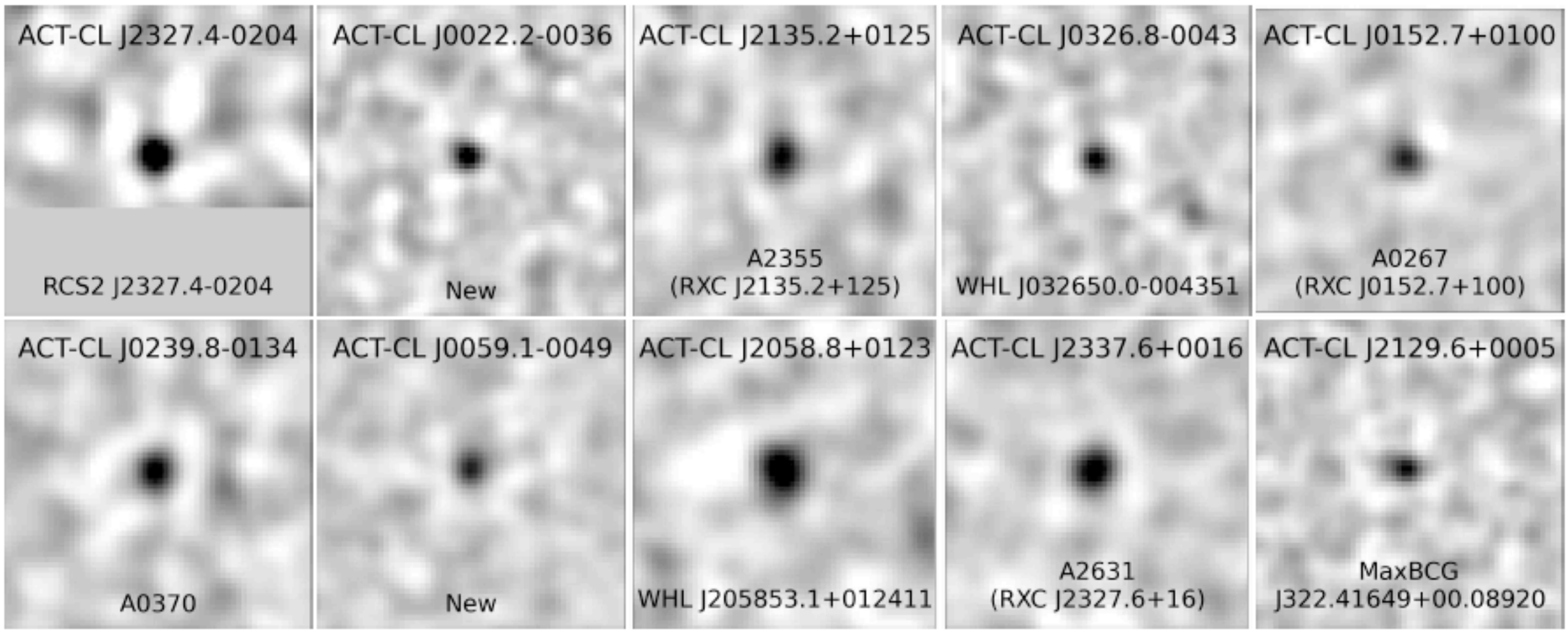

Figure 5. Postage stamp images (30′ on a side) for the 10 highest S/N detections in the catalog (see Table 7), taken from the filtered ACT maps. The clusters are ordered by detection S/N, from top left to bottom right, and each postage stamp shown is filtered at the scale which optimizes the detection S/N. Note that J2327.4−0204 is at the edge of the map. The greyscale is linear and runs from -350 μK (black) to +100 μK (white).

SZ-Mass Relation

$$\Psi_{\theta_{500}}(\boldsymbol{k}) = \frac{1}{\Sigma_{\theta_{500}}} \frac{B(\boldsymbol{k}) S_{\theta_{500}}(k)}{N(\boldsymbol{k})}$$ + Data(k) ⟶ Filtered SZ Decrement ΔT (Θ_{500}=5.9')

⟶ "Uncorrected" Central Compton y parameter

$$\widetilde{y}_0 \equiv \frac{\Delta T}{T_{\rm CMB}} f_{\rm SZ}^{-1}(m=0, z=0)$$

Scaling Relation

$$\widetilde{y}_0 = 10^{A_0+A} E(z)^2 (M/M_{\rm pivot})^{1+B_0+B} \times Q\left[\left(\frac{1+z}{1.5}\right)^C \theta_{500}/m^{C_0}\right] f_{\rm rel}(m,z).$$

A0, B0, C0 -- Universal Pressure Profile (UPP) based scaling parameters (Arnaud 2010)

Relativistic correction (~6%)

Q function "corrects" for fixed angular scale filter on a UPP profile of different scale

$$Q(\theta) = \int \frac{d^2k}{(2\pi)^2} \Psi(\boldsymbol{k}) B(\boldsymbol{k}) \int d^2\theta' \; e^{i\boldsymbol{\theta'}\cdot\boldsymbol{k}} \tau(\theta'/\theta)$$

Q is a fixed function

Comparison to X-ray Masses

Reasonable agreement with UPP masses (maybe not surprising given that UPP come from X-ray?)

Errors are large though

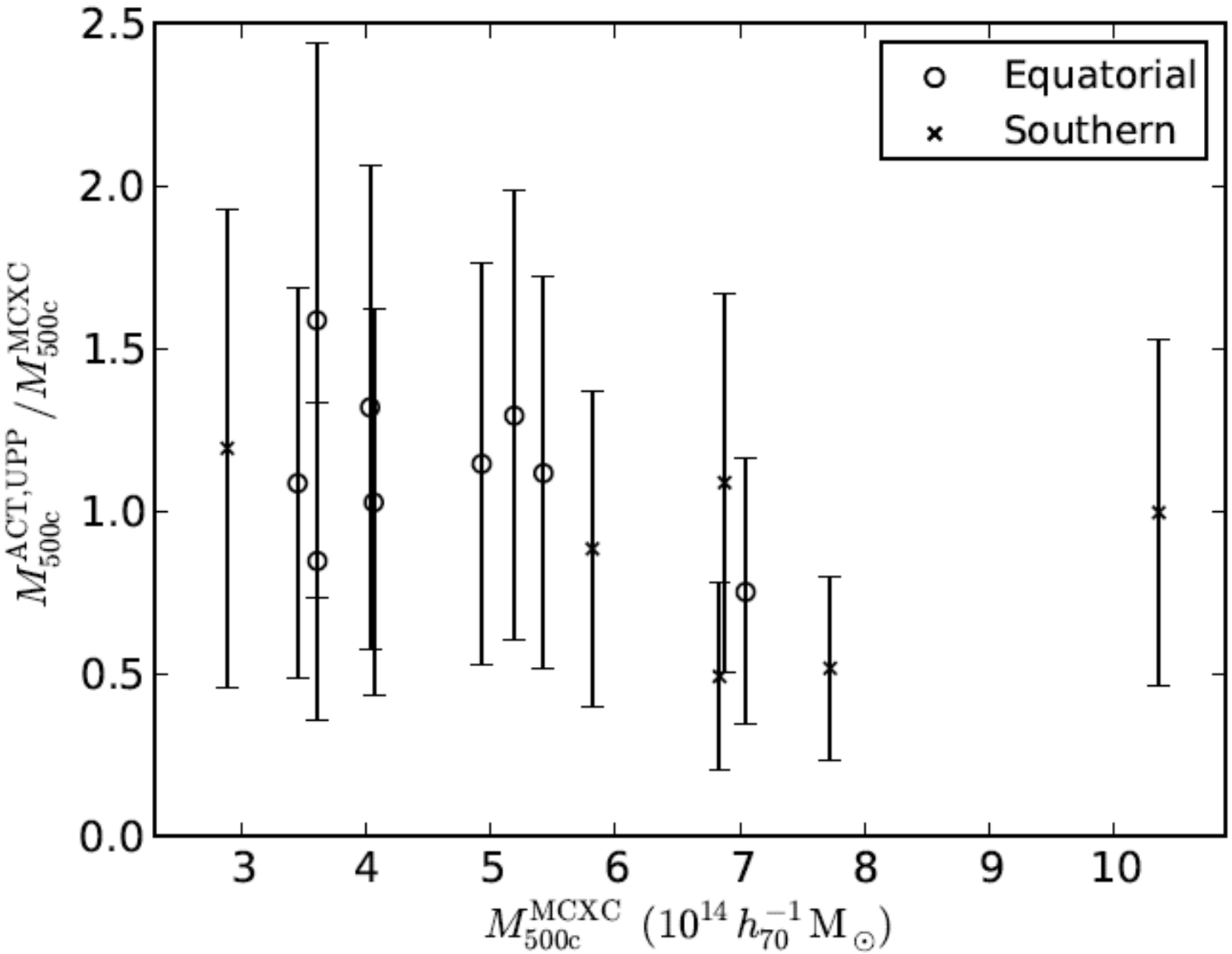

Figure 13. Ratio of ACT SZ determined masses to X-ray luminosity based masses from the MCXC. ACT masses assume the UPP scaling relation parameters. Error bars on mass include uncertainty from the ACT SZ measurements, and 50% uncertainty on MCXC masses. The weighted mean ratio is 1.03 ± 0.19 for the Equatorial clusters and 0.83 ± 0.13 for the full sample.

Full Scaling Relation Table

Description	A_m	B	C	$\sigma_{\rm int}$
Universal Pressure Profile (UPP)	0	0	0	0.20[a]
Models (§3.4)				
B12	-0.17 ± 0.06	-0.00 ± 0.20	-0.04 ± 0.37	0.20
Nonthermal20	-0.29 ± 0.06	0.00 ± 0.20	0.67 ± 0.47	0.21
Adiabatic	-0.02 ± 0.06	-0.08 ± 0.20	0.10 ± 0.43	0.21
Dynamical mass data (§3.5)				
All clusters	-0.21 ± 0.21	0.03 ± 0.51	0	0.31 ± 0.13
Excluding J0102	-0.11 ± 0.15	-0.28 ± 0.35	0	0.19 ± 0.10
Full cosmological MCMC (§5.3)				
ΛCDM model	-0.45 ± 0.19	0.36 ± 0.36	0.43 ± 0.62	0.42 ± 0.19
wCDM model	-0.46 ± 0.21	0.36 ± 0.35	0.34 ± 0.65	0.45 ± 0.20

Cosmology

Parameters

Cosmo: Ω_m, σ_8, ...

Scaling: A, B, C, σ, ...

Number counts in observable space

SZ selection function

$$n(\mathbf{x}|\boldsymbol{\theta},\boldsymbol{\psi},\beta^{\rm dyn}) = S(\widetilde{y_0},z,\delta\widetilde{y_0})\times$$
$$\int d\widetilde{y_0}^{\rm tr} d\widetilde{m}^{\rm tr} dz^{\rm tr} P(\mathbf{x}|\widetilde{y_0}^{\rm tr},\widetilde{m}^{\rm tr},z^{\rm tr},\beta^{\rm dyn}$$
$$n(\widetilde{y_0}^{\rm tr},\widetilde{m}^{\rm tr},z^{\rm tr}|\boldsymbol{\theta},\boldsymbol{\psi}). \quad (2$$

Poisson-based Likelihood confrontation with measurements

Binned Data

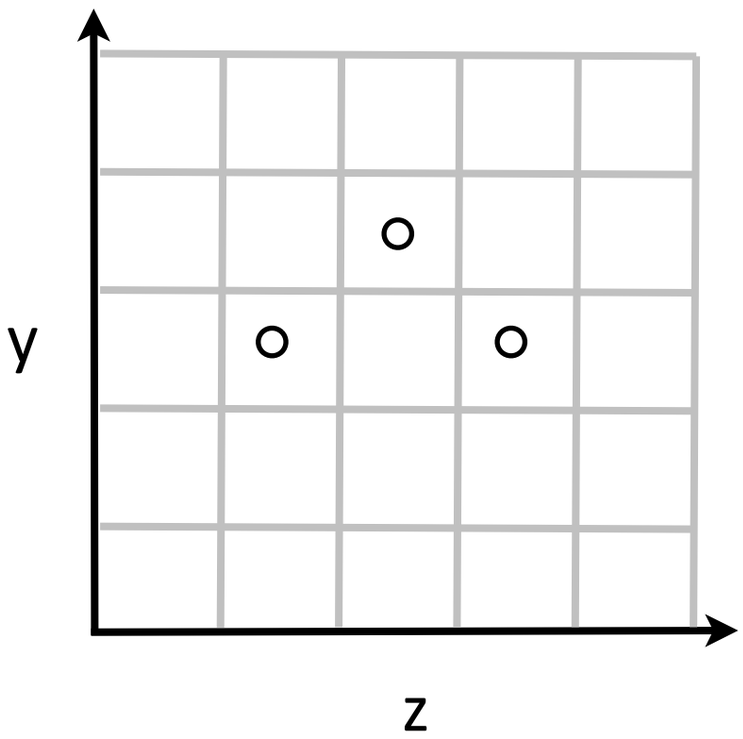

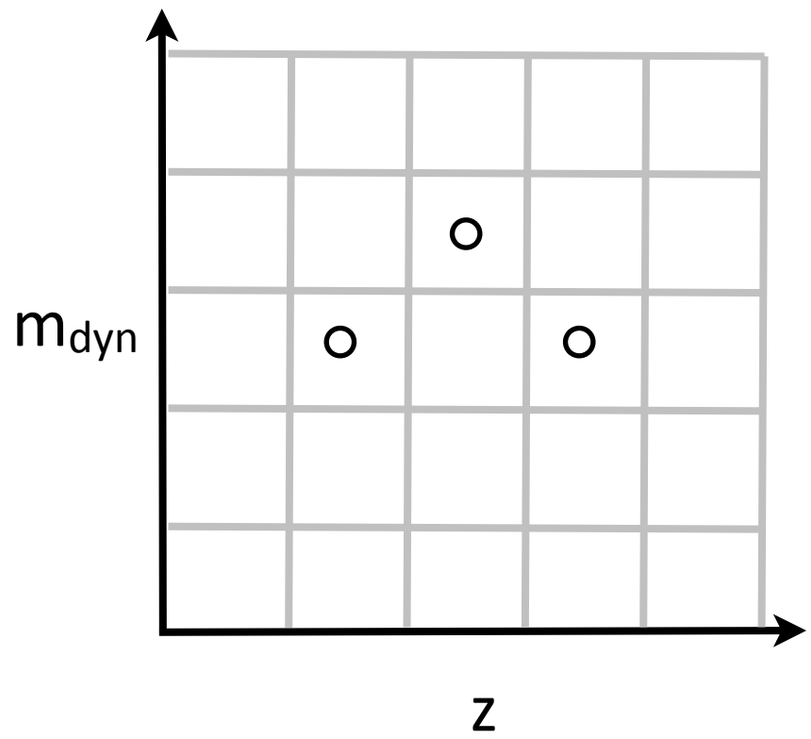

Cosmology

15 equatorial clusters with S/N>5.1; 0.2<z<1.4

+ 7 southern clusters with S/N>5.7; 0.314<z<1.4; and measured m_{dyn}

Marginalize over cosmo and scaling relations, including 15% bias in dynamical mass.

Result:

Constraints favoring high σ_8 because of an exceptional sample (El Gordo, Bullet...) but still consistent with upper half of WMAP volume

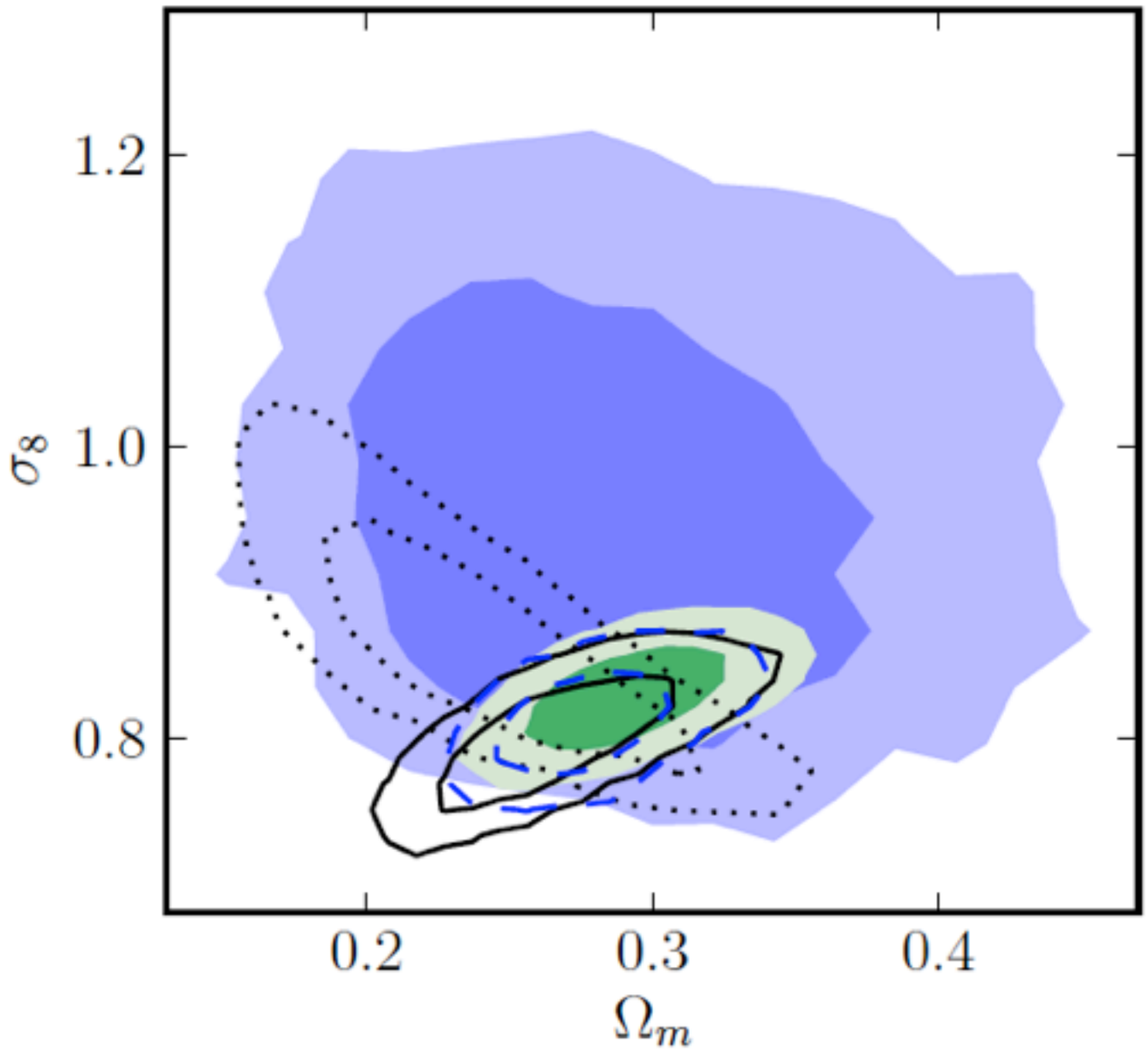

Figure 16. Constraints on ΛCDM cosmological parameters from Equatorial and Southern clusters. Results from ACTcl(dyn)+BBN+H0 (violet contours), and WMAP7+ACTcl(dyn) (green contours), which both include full marginalization over scaling relation and dynamical mass bias parameters, may be compared to WMAP alone (solid black lines). Dotted line shows constraints for ACTcl+BBN+H0, using the same cluster sample but with the scaling relation fixed to the central values obtained from the dynamical mass fit of Section 3.5; note the similarity to contours in Figure 14 obtained for Equatorial SZ data with B12 fixed scaling relation parameters. Dashed blue line shows WMAP7+ACTcl(dyn), with full marginalization over scaling relation parameters but with β^{dyn} fixed to 1.33.

Follow-up From Southern and Northern Observatories

SZA follow-up of New Massive z=0.82 Cluster

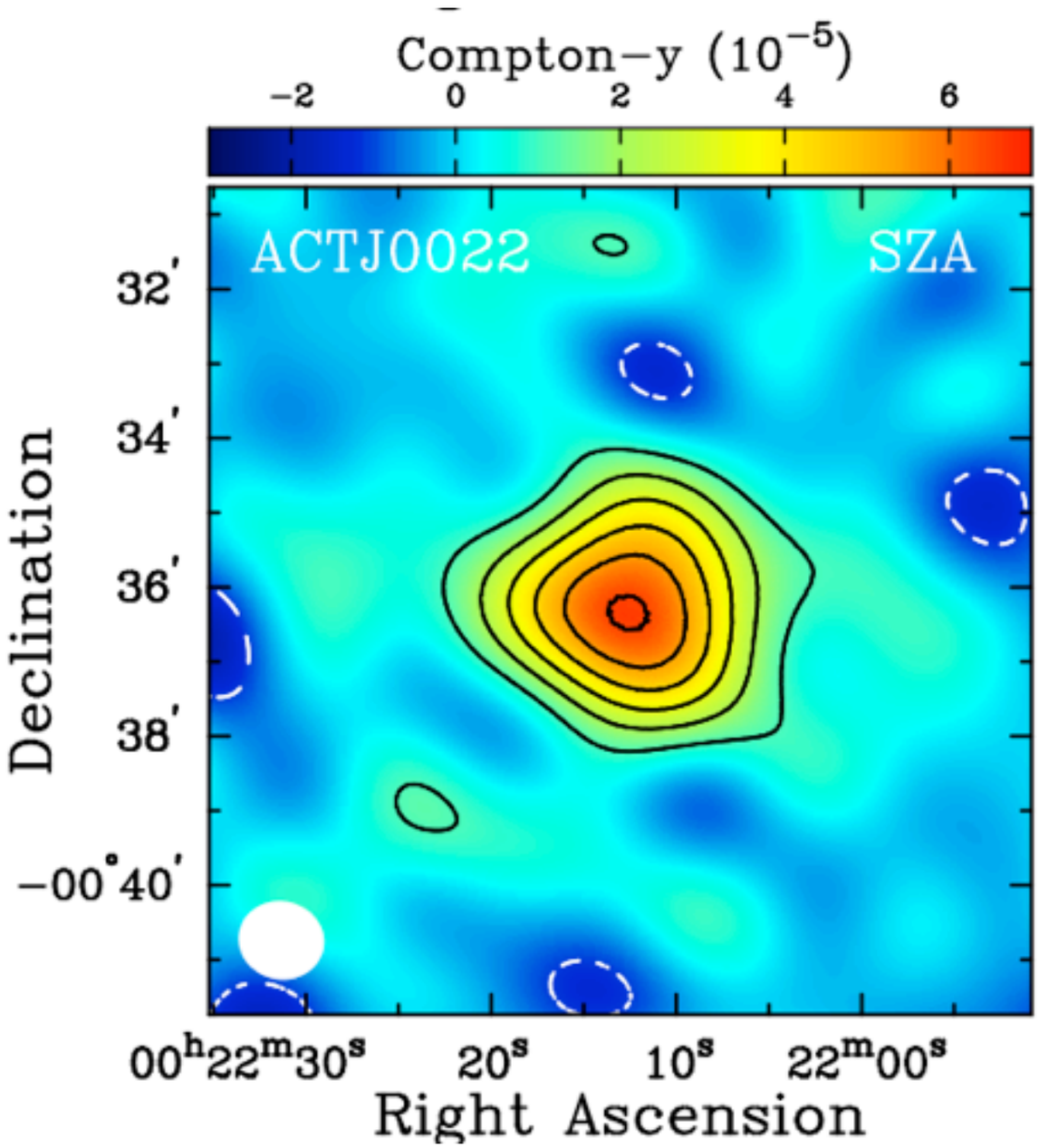

Reese et al (2011), 1108.3343

CARMA

Host of millimeter facilities in the north for detailed SZ studies.

Working To Constrain Inner and Outer Scales with SZA+ACT+Planck

More SZA data on all S/N>6 Equatorial Clusters

Reese et al 2013, in prep

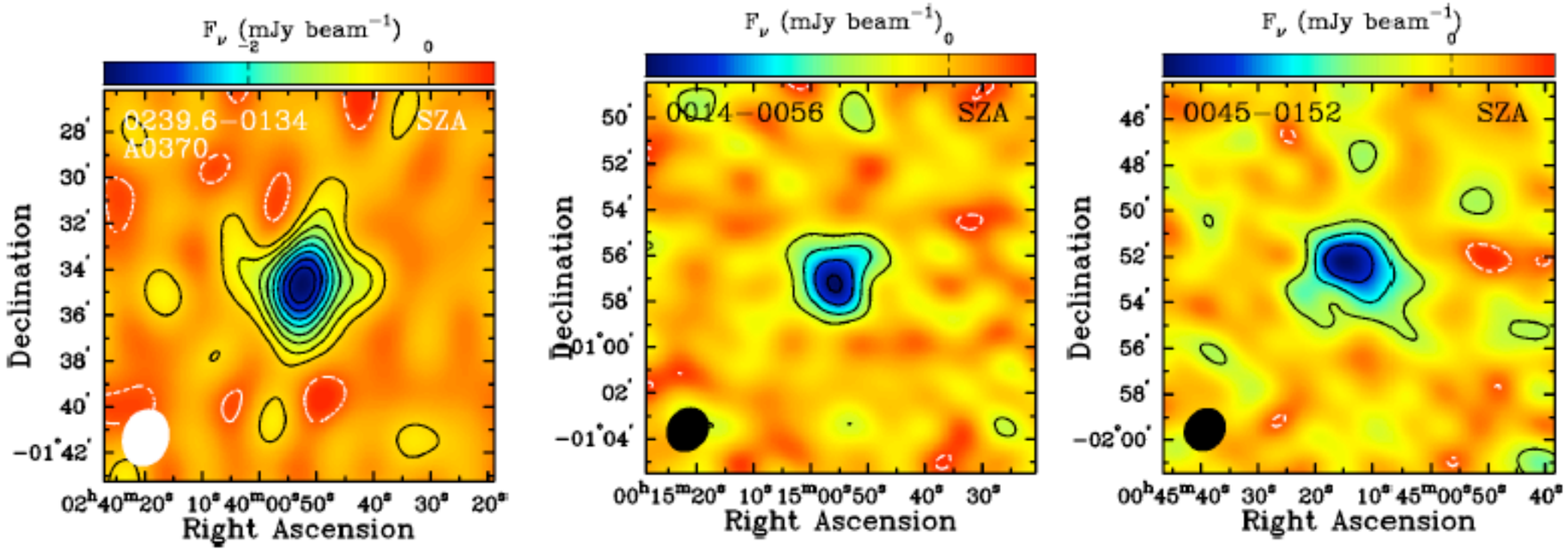

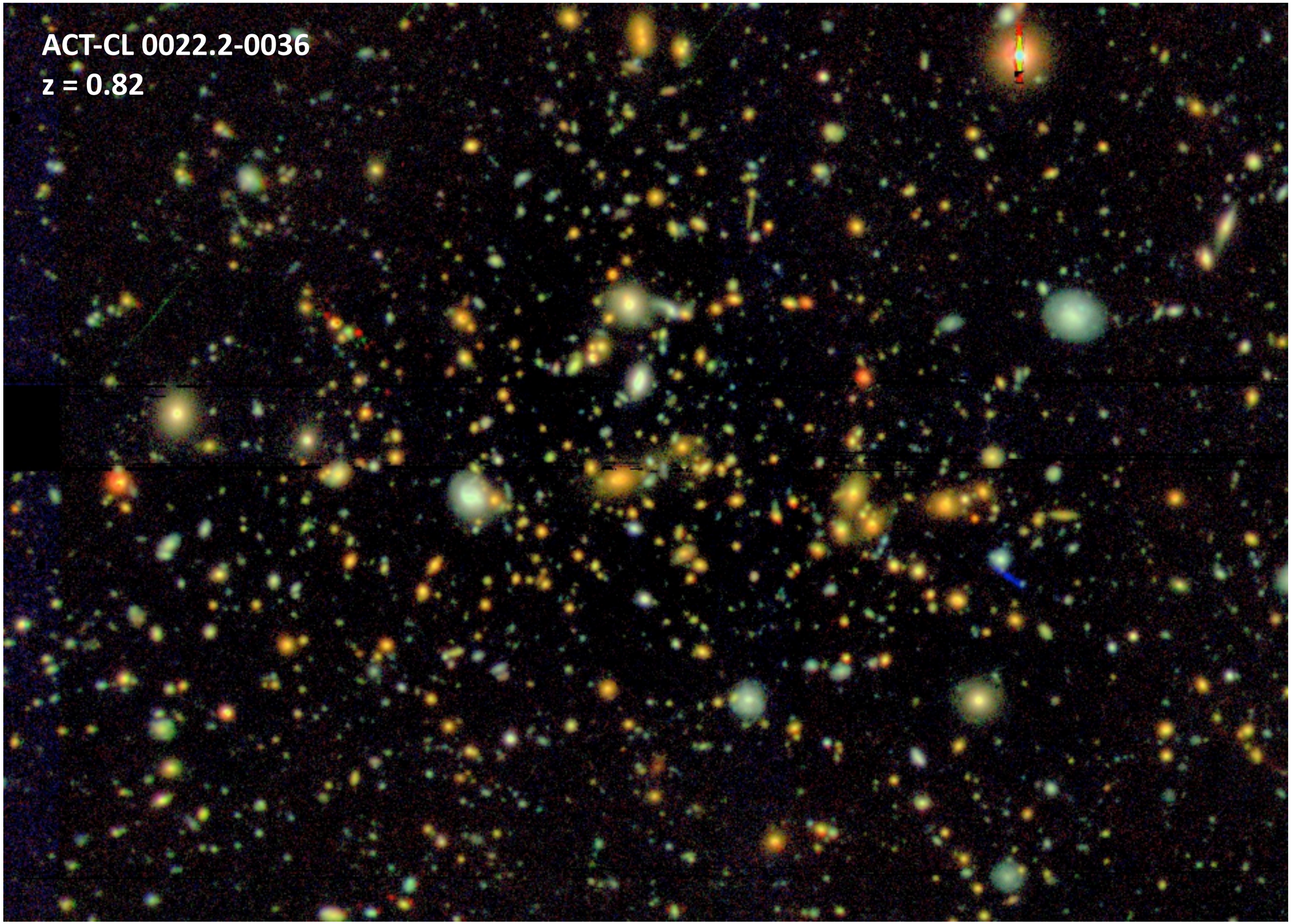

Subaru Lensing Study of ACT Equatorial Cluster

Miyatake et al 2012

Study of SZ vs Optical Richness

Sehgal et al 2012

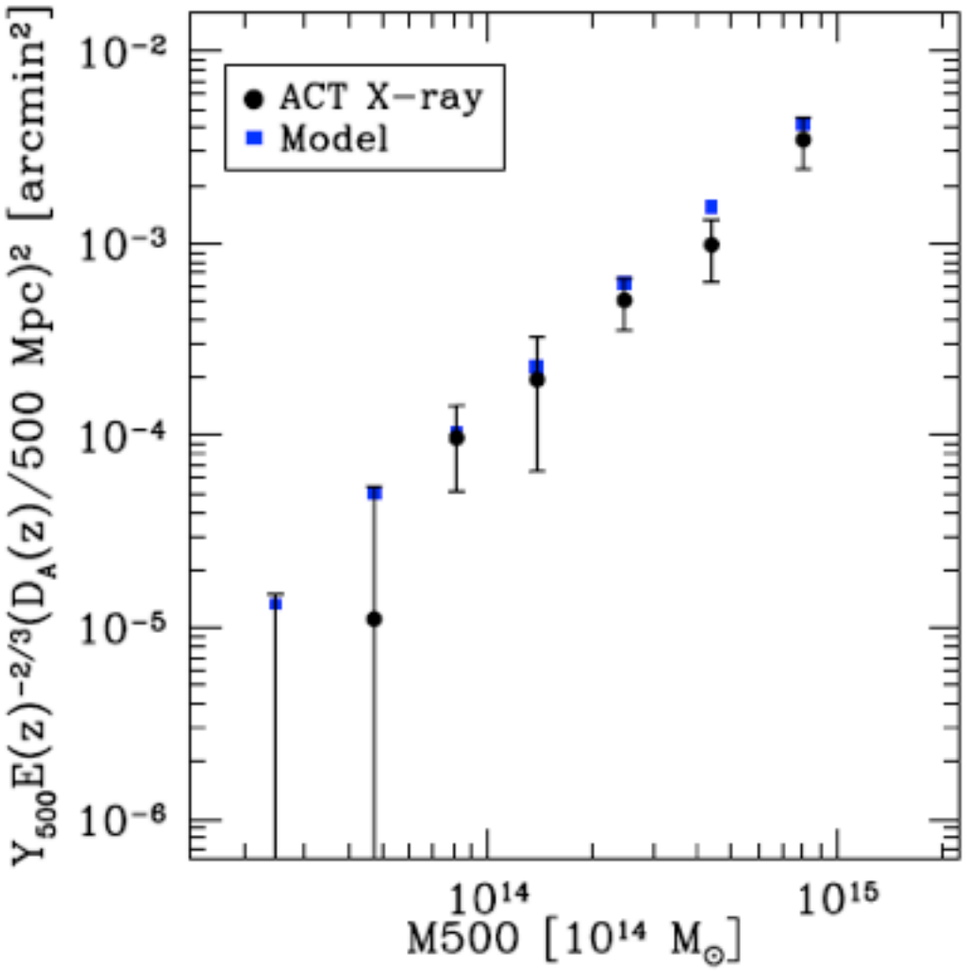

FIG. 4.— Measured Y_{500} values for 52 MCXC X-ray-selected clusters (Piffaretti et al. 2011) that fall within the ACT equatorial and southern survey regions (black circles). Also shown are expected Y_{500} values based on measured cluster X-ray properties (blue squares). A cluster profile model from Arnaud et al. (2010) was assumed for determining both measured and expected Y_{500} values.

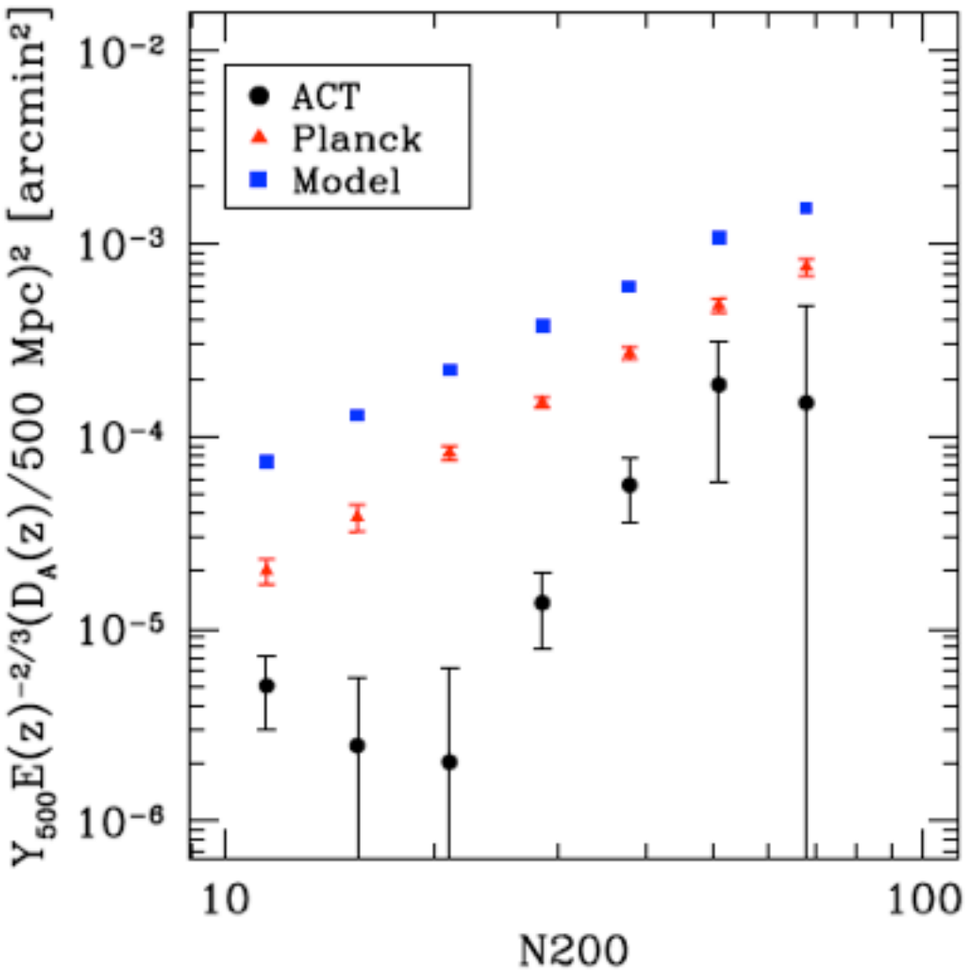

FIG. 5.— Measured Y_{500} values for 474 MaxBCG optically-selected clusters that fall within the ACT equatorial survey region (black circles). Expected Y_{500} values are shown as blue squares. Both measured and expected values assume the $N_{200m} - M_{500c}$ relation from Rozo et al. (2009) and the Arnaud et al. (2010) cluster profile. Red triangles are the measured values from the *Planck* satellite for a sample of 13,104 MaxBCG clusters (Planck Collaboration et al. 2011c).

El Gordo, El Gordo, El Gordo

345GHz and 2.1GHz imaging of "El Gordo"

LABOCA 345GHz

+

ACT Contours

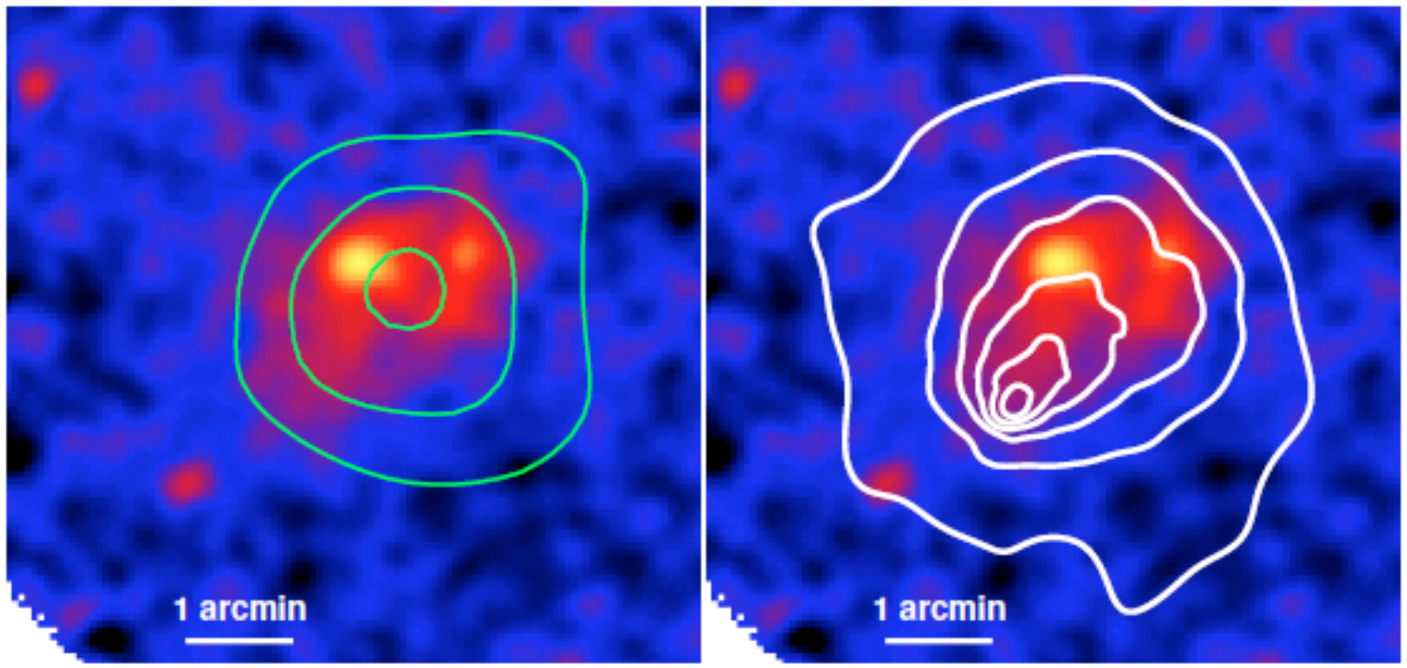

LABOCA 345GHz

+

ACT Contours

ATCA 2.1 GHz

+

LABOCA

contours

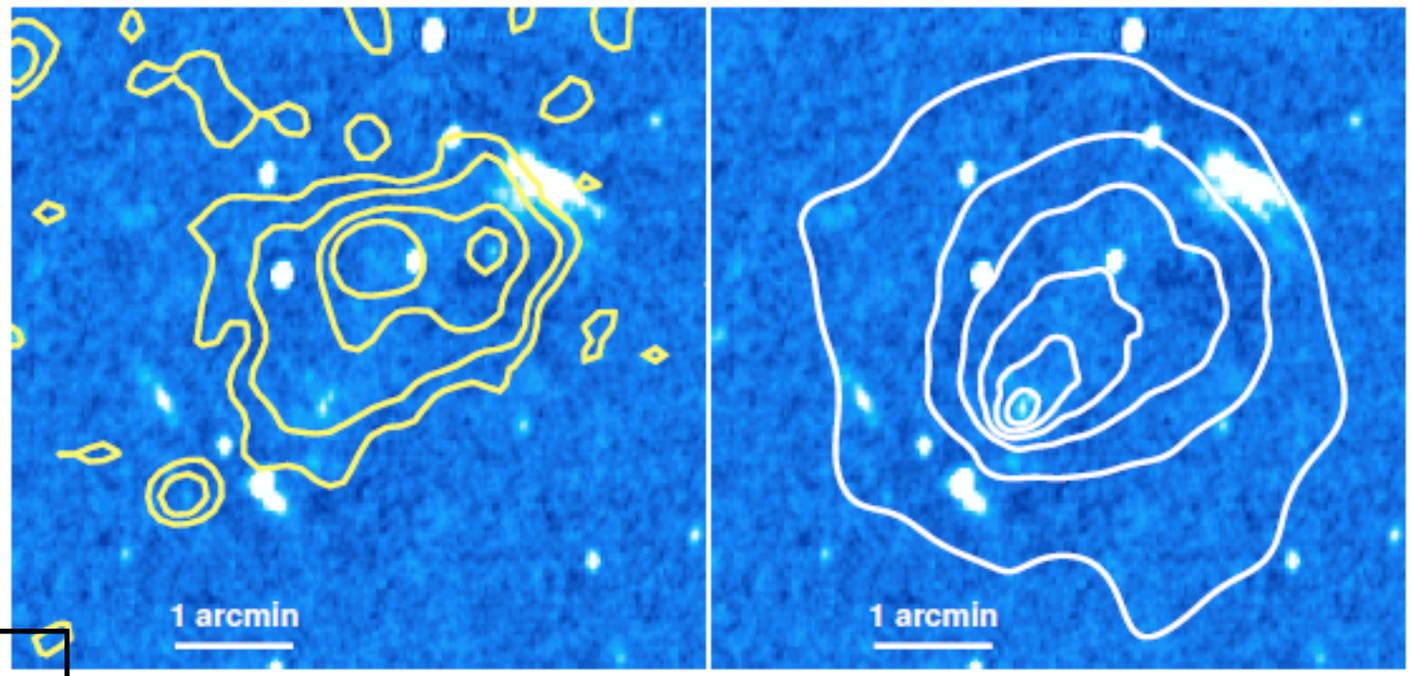

ATCA 2.1 GHz

+

Chandra

contours

- SZE signal is resolved into ``wake'' morphology

Lindner et al. (2013, in prep)

610MHz radio halo morphology traces El Gordo's wake

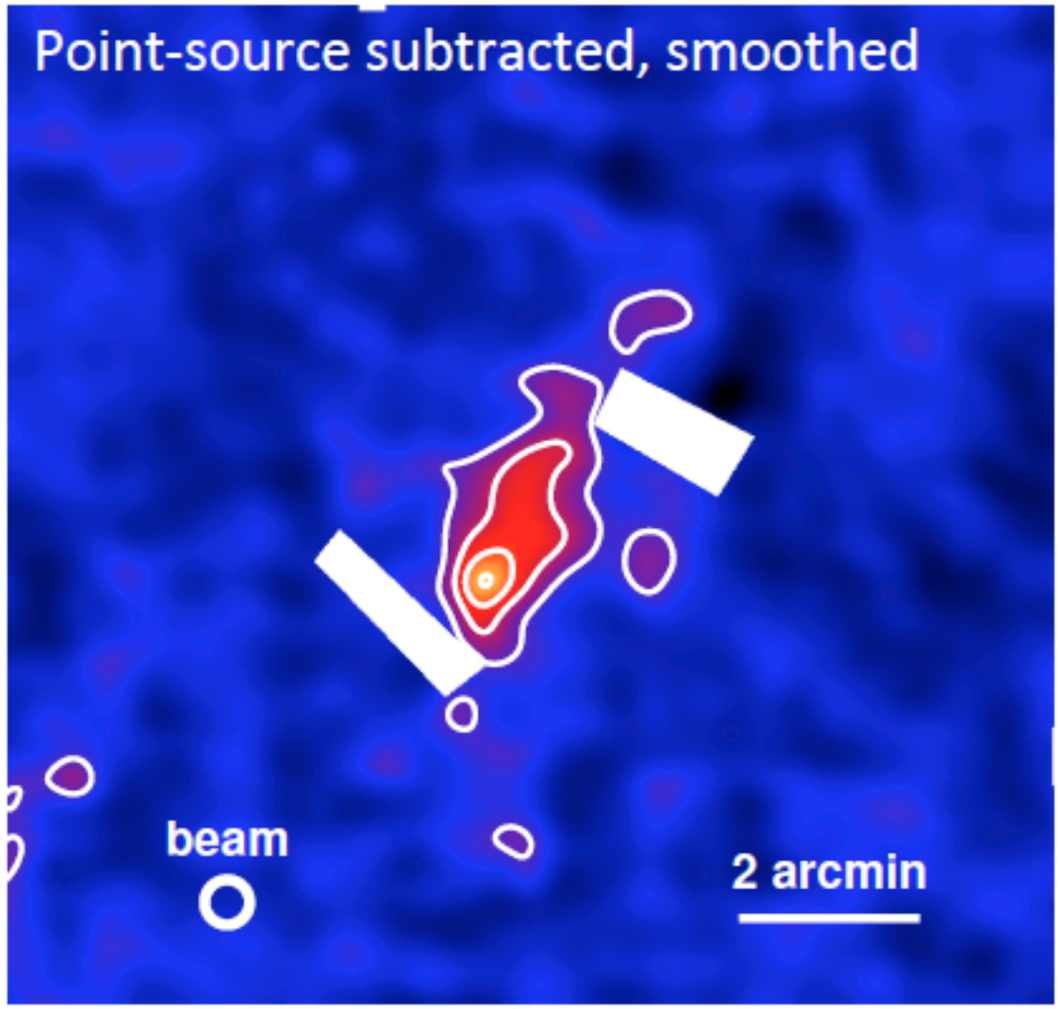

GMRT 610MHz

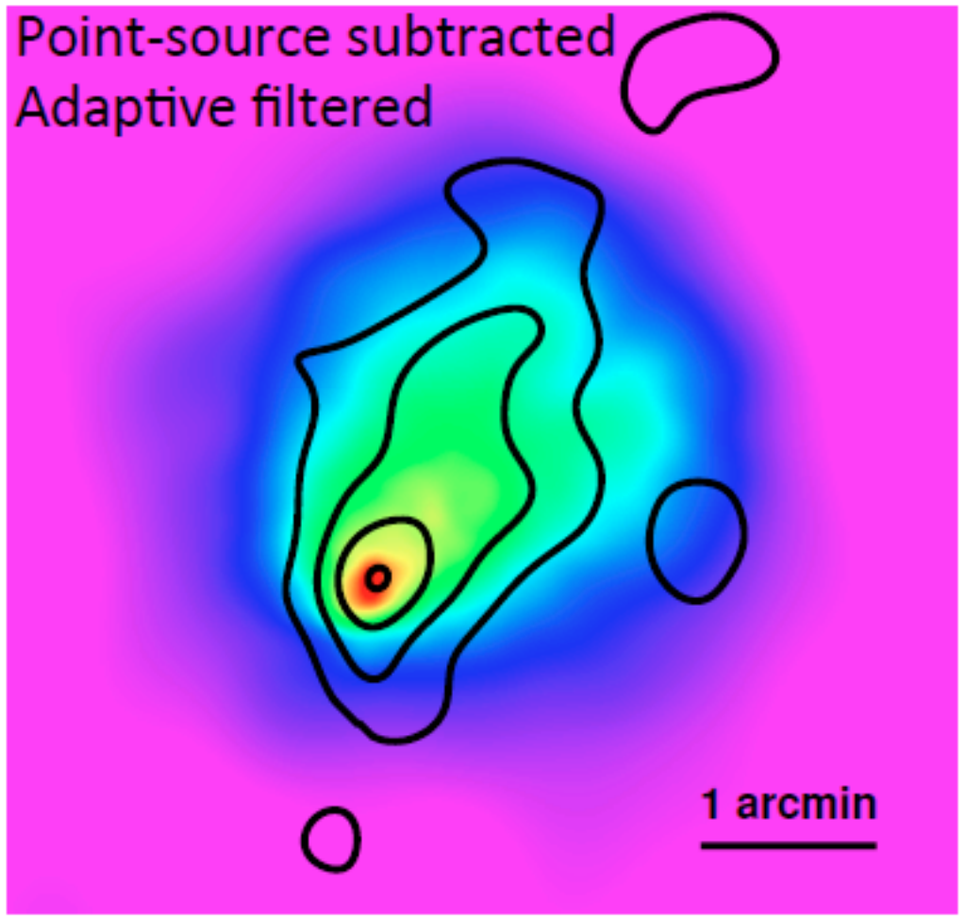

Chandra X-ray

- High energy electrons revealed by halo may affect observed SZE
- Halo emission peak may be result of diffusive shock acceleration

Lindner et al. (2013, in prep)

Working To Constrain Inner and Outer Scales with SZA+ACT(+Planck)

More SZA data on all S/N>6 Equatorial Clusters

Reese et al 2013, in prep

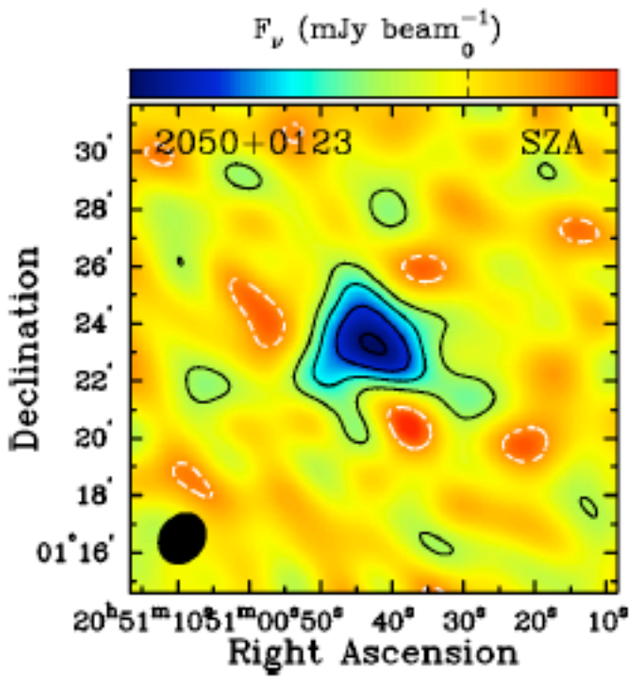

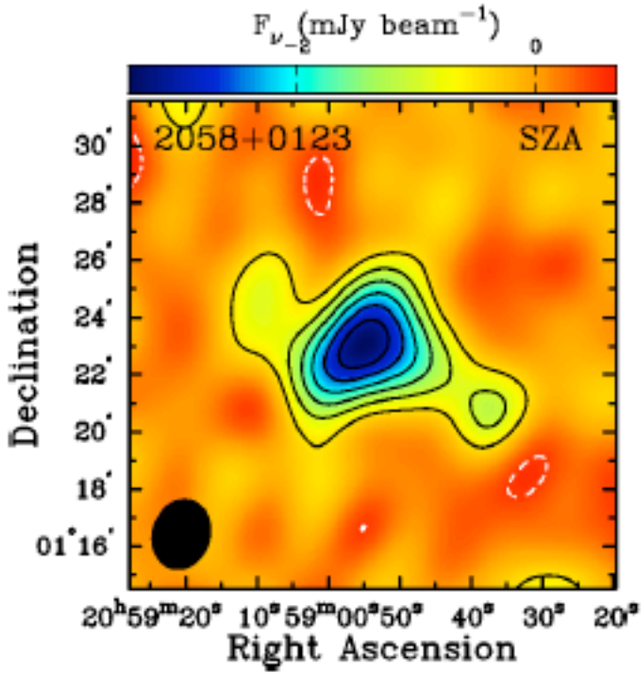

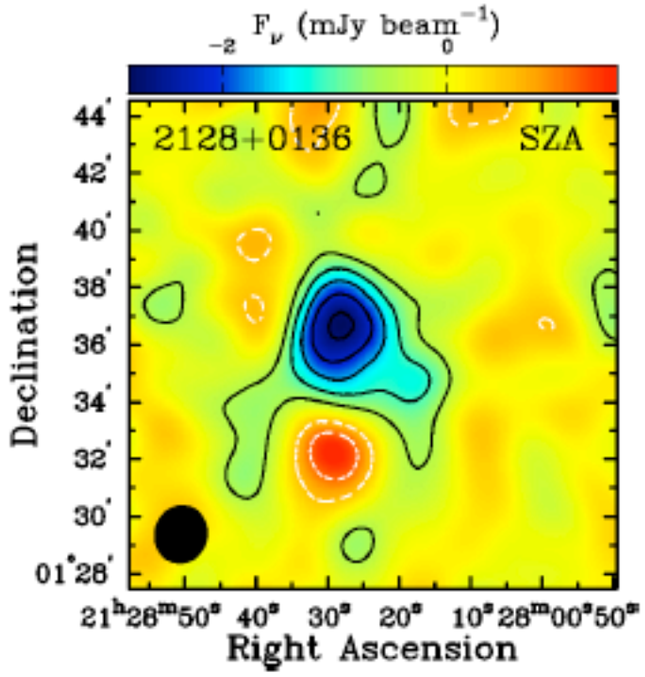

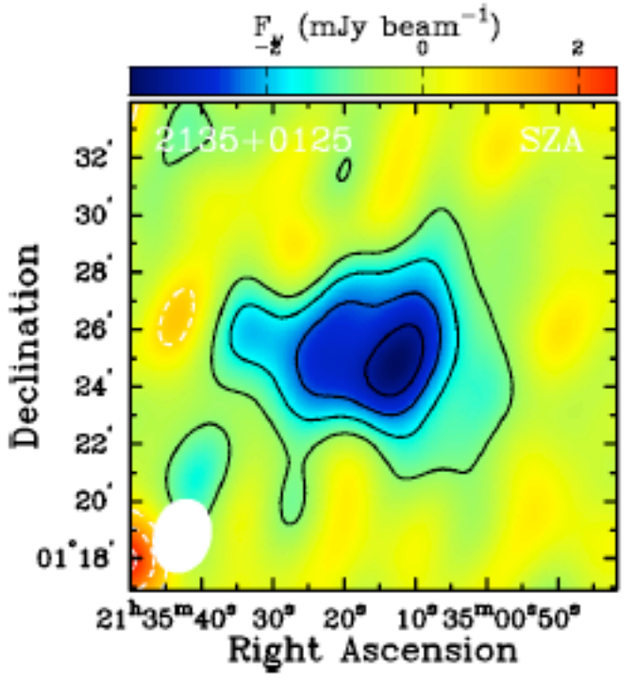

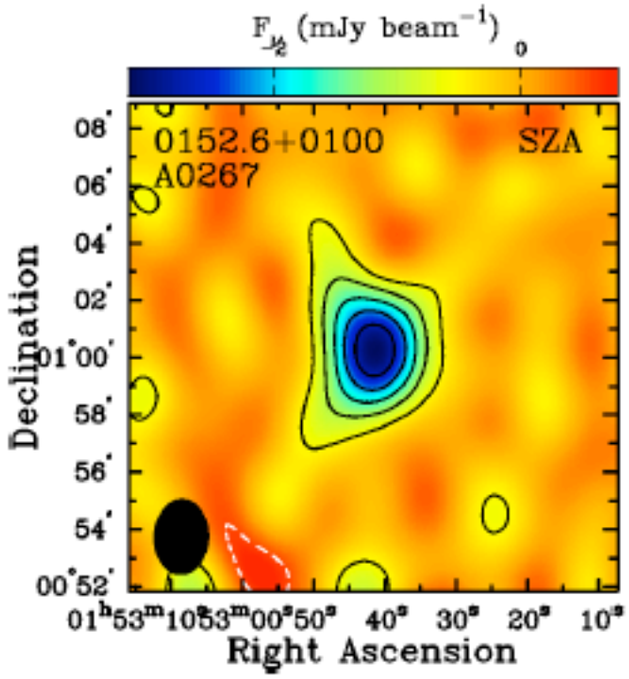

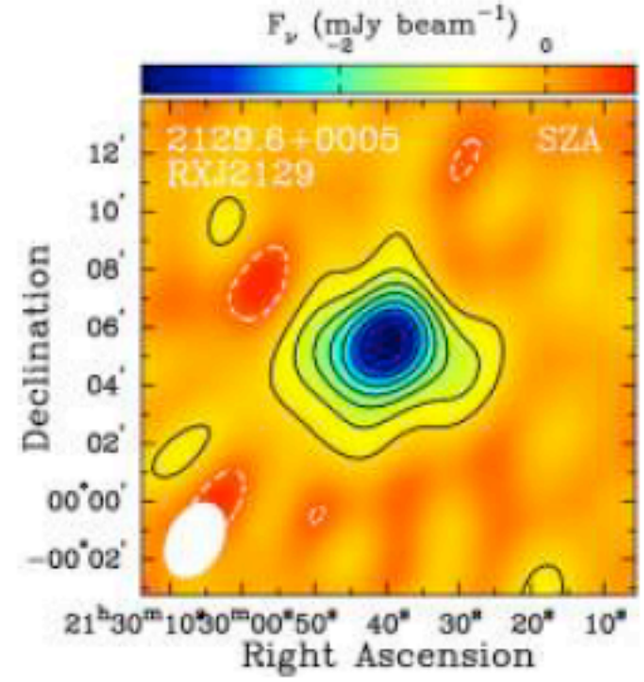

Skewness

Wilson, Hill, Sherwin et al 2012

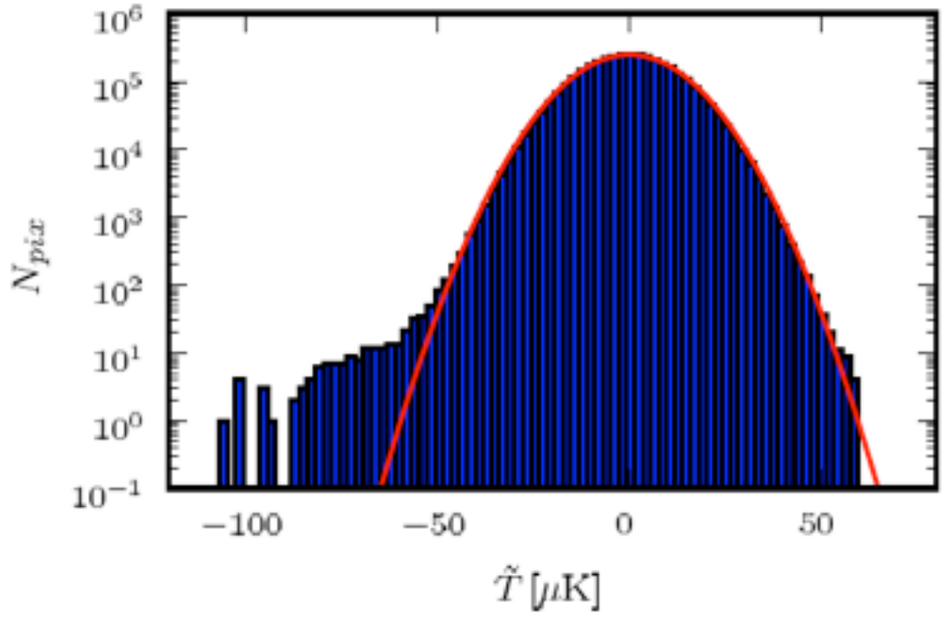

FIG. 2. Histogram of the pixel temperature values in the filtered, masked ACT CMB temperature maps. A Gaussian curve is overlaid in red.

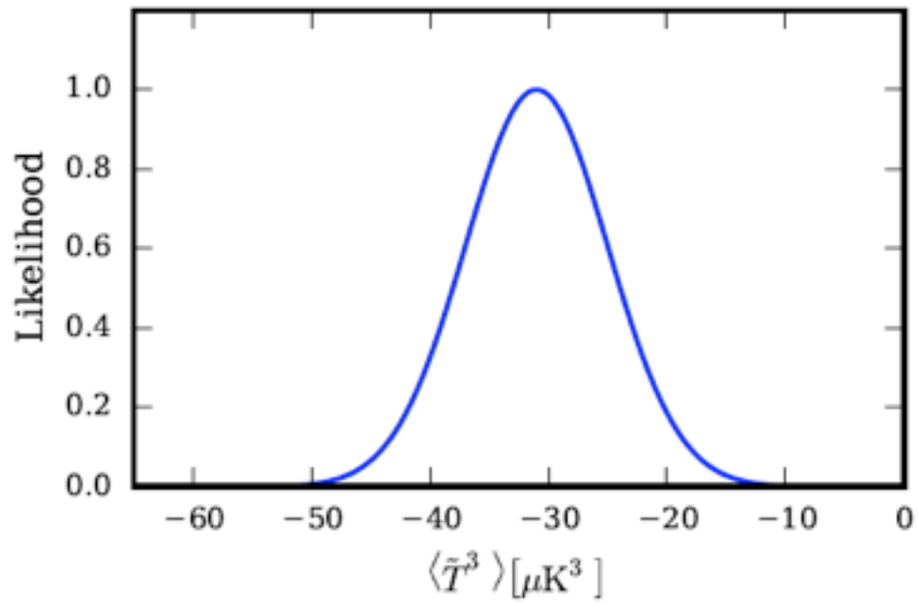

FIG. 3. Likelihood of the skewness measurement described in the text (with Gaussian statistics assumed).

$$\langle \tilde{T}^3 \rangle^{\rm th}(\sigma_8) = \langle \tilde{T}^3 \rangle^S \left(\frac{\sigma_8}{0.8}\right)^{\alpha_3}$$

$\alpha_3 \approx 11$ (depends on SZ model)

- Contribution to skewness mainly from low redshift massive clusters (unlike power spectrum).
- Weak dependence on Ω_m.

σ_8 = 0.78 +/- 3% statistical +/- 3% systematic

Should we use this (or other probes) to constrain cluster physics?